ANALYTICAL METHOD FOR ANALYZING C-CHANNEL STIFFENER MADE OF LAMINATE COMPOSITE

by

TATTCHAPONG KUMTON

Presented to the Faculty of the Graduate School of

The University of Texas at Arlington in Partial Fulfillment

of the Requirements

for the Degree of

MASTER OF SCIENCE IN AEROSPACE ENGINEERING

THE UNIVERSITY OF TEXAS AT ARLINGTON

December 2012

ACKNOWLEDGEMENTS

I would like to thank to my supervising professor Dr. Wen S. Chan for his guidance, patience and encouragement during of this thesis. I would like to thank Dr.Nomura and Dr. Adnan for serving as members of my committee.

Finally, I would like express my gratitude towards my parent, my beloved brothers and sister, my girlfriend, and my friends for their never-ending support and encouragement throughout my life.

November 19, 2012

ABSTRACT

ANALYTICAL METHOD FOR ANALYZING C-CHANNEL

STIFFENER MADE OF LAMINATE

COMPOSITE

Tattchapong Kumton, M.S.

The University of Texas at Arlington, 2012

Supervising Professor: Wen S. Chan

Composite materials play the important role in the aviation industry. Conventional materials such as aluminum were replaced by composite material on the main structures. The objective of this study focuses on development of analytical method to analyze the laminated composite structure with C-channel cross-section.

A lamination theory base closed-form solution was developed to analysis ply stresses on the C-channel cross-section. The developed method contains the effects of coupling due to unsymmetrical of both laminate and structural configuration levels. The present method also included the expression of the sectional properties such as centroid, axial and bending stiffnesses of cross-section. The results obtain from analytical method showed an excellent agreement with finite element results.

TABLE OF CONTENTS

LIST OF ILLUSTRATIONS

Figure Page

LIST OF TABLES

CHAPTER 1

INTRODUCTION

1.1 Composite Material Overview

Composite materials have been used for many years. They are very popular in many industries because they have more advantages than traditional materials such as high specific strength and stiffness, corrosion resistance, lightweight and the ability to tailor. Composite materials are used as component of many types of structure especially in aviation industrial. At the first time, composite materials were used as a secondary structure of aircrafts. The progressing in technology also led composite materials dramatically grows. The composite materials were used on primary structure. Nowadays, 80% of aircrafts composed of composite materials. Not only aviation industries but also the everyday applications such as automobile, sport equipment, and civil structure used composite materials.

In the aviation industries, most of structures and components such as tails, wings, fuselage and propellers are made of composite material. The laminated composite beams and plates are often used because they can be design to meet the specific requirement of each application. Due to each part has different function, so each of them must be deal with different kind of loads and environment conditions such as tension, compression, pressure and temperature. The designer designs and optimizes the best solution in term of quality and economy.

The laminated composite can be able to design to meet with the requirement, but there have to know the properties and behavior of material under various kinds of loads. The temperature is one of important factors that must be considered. The study of laminated composite behavior under thermal environment is necessary for engineer. The aircraft

structures are composed of many pieces of laminate composite beam and plate. The preliminary design needs to estimate the induced load and effect on laminate composite.

There have many 3D engineering programs that were designed to handle with this problem such as ANSYS, SOLIDWORK and Pro/ENGINEER. Those programs can help engineer to model the structure and apply loads on the model, and then obtain the result. Those programs also help to reduce time, cost and optimize quality of structure to meet the requirement in aircraft design. Although, those engineering programs are very helpful for engineer to get the result, the preliminary calculation also needs to estimate the basic information before modeling. The analytical method is developed in order to estimate the solution.

1.2 Literature Review

There have many research studies on composite material. Most of them focus on laminate composite thin-wall structure under various types of load. The study of composite material begins with the simple structure.

Vasiliev [1] studied on standard structure element such as this walls beam, plates, panels and shells. The engineering mechanics is based on a system of hypotheses specific for each typical element. The engineering methods are developed to calculate stress loads, and behavior of structure. Barbero [2] provided a simple preliminary-design procedure that summarizes and complements for beam-design and also novel methodology for analysis thin-walled composite section. In addition, He provided a powerful method for preliminary design to analysis the composite plate and stiffened panel, and shells structure. Complex analytical or numerical procedures have not been included. His method can calculate the center of gravity of cross-section, axial, bending, and torsion stiffness, and shear of open sections.

Chan and Demirhan [3] developed model for analytical closed-form to calculate the bending stiffness of laminated composite circular tube made of fiber-reinforced composites. The analysis based upon modified laminated plate and shell theories. The approaches also include

effect of ply orientation due to radius curvature. Su et al [4] develops the closed-form solution for the laminated composite circular tube, and rectangular beam and also analysis the in-plane stress and inter-laminar shear stress through the thickness. The development was based on lamination theory, parallel axis theory, and laminated plate approach. The parametric study is conducted to study the stacking sequence and fiber orientation effect. Nguyen et al [5] investigates the laminate stresses in a curved laminated beam under pure bending moment. The closed-form was developed to understanding the characteristics of a curved laminate and calculates the radial stress and tangential stress effect due to curvatures, stacking sequence and fiber orientation.

Syed and Chan [6] investigated the behavior of hat-section reinforce composite beam due to various loads. A closed form solution was developed for composite beam using lamination theory and translation of axis theorem. The model was simplified from three-dimensional into two-dimensional plate. The researcher also considers the effect of induced in-plane deformation due to bending for unsymmetrical cross-section. Jung and Lee [7] were interested in thin wall composite I-beam and perform a closed-form analysis. Parambil [8] developed an analytical method to analyze the stresses of laminated composite I-beam. An analytical expression is developed for calculate sectional properties such as centroid, equivalent axial and bending stiffnesses, and also analysis of stresses of I-beam. This study also includes the effect of the symmetrical and unsymmetrical laminated and parametric. Rios [9] started his study on simple laminate composite plate. The research was extending to develop sectional properties of laminated composite with a stiffener boned together, both stiffener aligned and unaligned with centerline of laminate width. The analysis focuses on centroid location, axial and bending stiffnesses, and the ply stresses of the whole structure. In addition his work extends to analysis a z-stiffener, circular cross-section beam and airfoil composite beam. The results were compared with the finite element method.

1.3 Objective and Approach

The main objective of this research is to study the laminate composite beam with C-Channel cross-section under thermal environment. The analytical method is developed based on classical laminate theory to estimate stress on each lamina. The C-channel beam composed of three composite laminated plates that are considered as narrow beam. The analytical method also calculates the sectional properties such as centroid of cross-section, axial and bending stiffness. The analytical method is also developed to solve with the different laminate layup problem. ANSYS13.0 is use to model the 3D laminated composite with C-channel cross-section beam. The results from analytical method and finite element will be comparing.

1.4 Outline of the Thesis

Chapter 2 will review the basic knowledge of elastic mechanic and constitute equation. This chapter included the stress/strain relationship and transformation, classical lamination theory, and narrow/wide beam.

Chapter 3 describes the geometry of C-channel cross-section and development of the analytical method to calculate the sectional properties and ply stresses on cross-section.

Chapter 4 gives a detail of finite element method with ANSYS such as the modeling procedure, boundary condition and result collecting.

Chapter 5 lists the result for sectional properties and ply stresses in various cases.

Chapter 6 is conclusion and future work of the research.

CHAPTER 2

BASIC EQUATION FOR COMPOSITE LAMINATE BEAM

This chapter also refers to basic knowledge of stress/strain relationship general constitute equation, the general constitutive equation of laminate plate or know as classical laminate theory.

2.1 Stress Component

The general case of three-dimensional state of stress is shown in figure 2.1. There have uniformly stress distributed on each face and acting at the center of each face. The nine scalar stress components represent state of stress at a given point. They can be writing in matrix form as follow:

$$[\tau_{ij}] = \begin{bmatrix} \tau_{xx} & \tau_{xy} & \tau_{xz} \\ \tau_{yx} & \tau_{yy} & \tau_{yz} \\ \tau_{zx} & \tau_{zy} & \tau_{zz} \end{bmatrix} = \begin{bmatrix} \sigma_x & \tau_{xy} & \tau_{xz} \\ \tau_{yx} & \sigma_y & \tau_{yz} \\ \tau_{zx} & \tau_{zy} & \sigma_z \end{bmatrix} \quad (2.1)$$

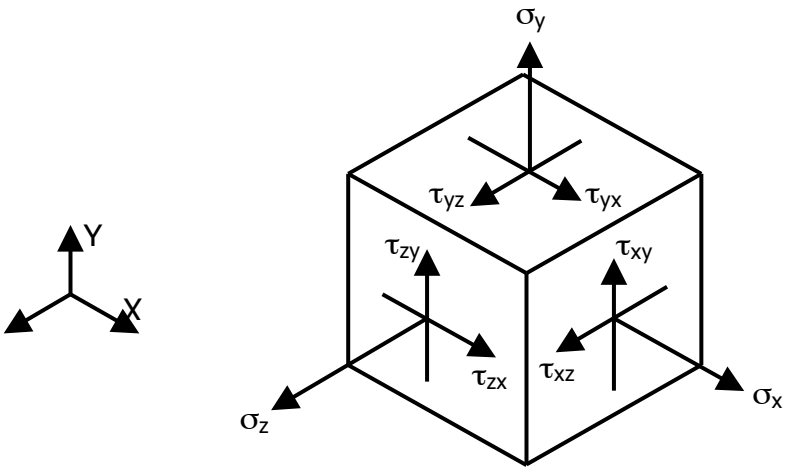

Figure 2.1 Element subjected to three-dimensional stress

The double subscript notation is interpreted as follows: the first subscript represents the normal direction of the surface; the second one represents the direction of the stress itself. The repetative subscripts that represent normal stress, τ_{xx}, τ_{yy}, and τ_{zz}, can be simplify as σ_x, σ_y, and σ_z.

2.2 Generalized Hooke's Law

For a three-dimensional state of stress, there have six stress components express as linear function of six strain components [11]. Thus, the Hooke's law for any elastic material can be writes as follow:

$$\begin{bmatrix} \varepsilon_x \\ \varepsilon_y \\ \varepsilon_z \\ \gamma_{yz} \\ \gamma_{xz} \\ \gamma_{xy} \end{bmatrix} = \begin{bmatrix} S_{11} & S_{12} & S_{13} & S_{14} & S_{15} & S_{16} \\ S_{21} & S_{22} & S_{23} & S_{24} & S_{25} & S_{26} \\ S_{31} & S_{32} & S_{33} & S_{34} & S_{35} & S_{36} \\ S_{41} & S_{42} & S_{43} & S_{44} & S_{45} & S_{46} \\ S_{51} & S_{52} & S_{53} & S_{54} & S_{55} & S_{56} \\ S_{61} & S_{62} & S_{63} & S_{64} & S_{65} & S_{66} \end{bmatrix} \begin{bmatrix} \sigma_x \\ \sigma_y \\ \sigma_z \\ \tau_{yz} \\ \tau_{xz} \\ \tau_{xy} \end{bmatrix} \text{ or } [\varepsilon] = [S][\sigma] \tag{2.2}$$

Equation (2.2) can be rewritten as,

$$\begin{bmatrix} \sigma_x \\ \sigma_y \\ \sigma_z \\ \tau_{yz} \\ \tau_{xz} \\ \tau_{xy} \end{bmatrix} = \begin{bmatrix} C_{11} & C_{12} & C_{13} & C_{14} & C_{15} & C_{16} \\ C_{21} & C_{22} & C_{23} & C_{24} & C_{25} & C_{26} \\ C_{31} & C_{32} & C_{33} & C_{34} & C_{35} & C_{36} \\ C_{41} & C_{42} & C_{43} & C_{44} & C_{45} & C_{46} \\ C_{51} & C_{52} & C_{53} & C_{54} & C_{55} & C_{56} \\ C_{61} & C_{62} & C_{63} & C_{64} & C_{65} & C_{66} \end{bmatrix} \begin{bmatrix} \varepsilon_x \\ \varepsilon_y \\ \varepsilon_z \\ \gamma_{yz} \\ \gamma_{xz} \\ \gamma_{xy} \end{bmatrix} \text{ or } [\sigma] = [C][\varepsilon] \tag{2.3}$$

Where [S] is a compliance matrix.

Where [C], a stiffness matrix, is the inverse of [S] matrix

2.3 Coordinate System of Composite Laminate

Generally, composite laminate composed of many plies with difference fiber orientation that perfectly bonded together. Two coordinate systems, 1-2-3 coordinate and x-y-z coordinate, are used to define as local fiber orientation coordinate system and global coordinate system, respectively. The 1-coordinate system refers to fiber direction; the 2-coordinate system refers to

transverse direction of in-plane and the 3-coordinate system refers to direction that perpendicular to in-plane ply.

As mentioned above, the composite laminate is usually considered as thin plate, so the plane stress condition is enforced ($\sigma_3 = \tau_{13} = \tau_{23} = 0$). With this assumption, composite laminate coordinate is reduced from 3-D to 2-D (1-2 coordinate and x-y coordinate) as shown in figure 2.2.

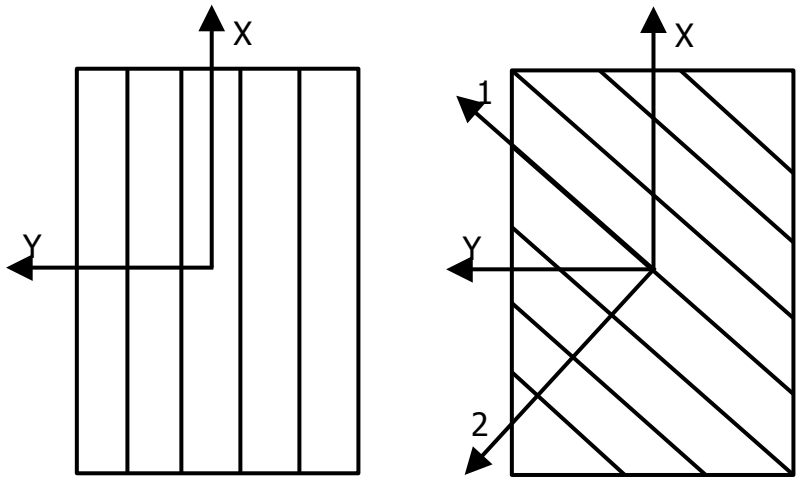

Figure 2.2 Global coordinates and material coordinate

2.4 Stress-Strain Relationship for Plane Stress Condition

For each layer, there have their orientations or material coordinates and treated as orthotropic material. The stress-strain relationship for 2-D composite laminate can be described in matrix form as follows:

$$\begin{bmatrix} \varepsilon_1 \\ \varepsilon_2 \\ \gamma_{12} \end{bmatrix} = \begin{bmatrix} S_{11} & S_{12} & 0 \\ S_{21} & S_{22} & 0 \\ 0 & 0 & S_{66} \end{bmatrix} \begin{bmatrix} \sigma_1 \\ \sigma_2 \\ \tau_{12} \end{bmatrix} \text{ or } [\varepsilon]_{1-2} = [S]_{1-2}[\sigma]_{1-2} \tag{2.4}$$

Inverse of reduced compliance matrix is reduced stiffness matrix.

$$\begin{bmatrix} \sigma_1 \\ \sigma_2 \\ \tau_{12} \end{bmatrix} = \begin{bmatrix} Q_{11} & Q_{12} & 0 \\ Q_{21} & Q_{22} & 0 \\ 0 & 0 & Q_{66} \end{bmatrix} \begin{bmatrix} \varepsilon_1 \\ \varepsilon_2 \\ \gamma_{12} \end{bmatrix} \text{ or } [\sigma]_{1-2} = [Q]_{1-2}[\varepsilon]_{1-2} \tag{2.5}$$

With elastic engineering properties, we can express component in [Q] matrix as:

$$Q_{11} = {}^{E_1}/_{(1 - v_{12}v_{21})} \tag{2.6}$$

$$Q_{22} = {}^{E_2}/_{(1 - v_{12}v_{21})} \tag{2.7}$$

$$Q_{12} = {}^{v_{21}E_1}/_{(1 - v_{12}v_{21})} = {}^{v_{12}E_2}/_{(1 - v_{12}v_{21})} \tag{2.8}$$

$$Q_{66} = G_{12} \tag{2.9}$$

2.5 Stress-Strain Transformation Matrices

Generally, global coordinate is used as the reference coordinate, so the local ordinate must be coincide with global coordinate. For two-dimension, fiber direction makes an angle (θ) with respect to global coordinate. In order to transform local stress/strain to global system, the transformation matrix is used as follows:

$$[\sigma]_{1-2} = [T_\sigma][\sigma]_{x-y} \tag{2.10}$$

$$[\varepsilon]_{1-2} = [T_\varepsilon][\varepsilon]_{x-y} \tag{2.11}$$

Where $[T_\sigma]$ and $[T_\varepsilon]$ are transformation matrices for stress and strain, respectively

$$[T_\sigma] = \begin{bmatrix} m^2 & n^2 & 2mn \\ n^2 & m^2 & -2mn \\ -mn & mn & m^2 - n^2 \end{bmatrix} \tag{2.12}$$

$$[T_\varepsilon] = \begin{bmatrix} m^2 & n^2 & mn \\ n^2 & m^2 & -mn \\ -2mn & 2mn & m^2 - n^2 \end{bmatrix} \tag{2.13}$$

Where $m = Cos\theta$ and $n = Sin\theta$ and θ is the fiber orientation of the ply

The reduced stiffness matrices [Q] are generally calculated in term of material coordinate. The 0° ply is considered as global coordinate system, while the other angles transform to coincide with global coordinate system. Then, the $[\mathrm{Q}]_{1-2}$ matrices also transform to $[\overline{\mathrm{Q}}]_{\mathrm{x-y}}$ matrices by using transformation matrices.

$$[\overline{\mathrm{Q}}]_{\mathrm{x-y}} = [\mathrm{T}_{\sigma}(-\theta)][\mathrm{Q}]_{1-2}[\mathrm{T}_{\varepsilon}(\theta)] \tag{2.14}$$

2.6 Classical Laminate Theory

The laminated composite is combined of several thin angle plies with perfectly bonded together as shown in figure 2.3. To analyze the behavior of laminated composite, the mid-plane of the laminated is selected as reference plane and treated laminated as single plate. Then, the strain of any point can be calculated in term of the mid-plane strains and curvatures in global coordinated system. The stacking sequence of a laminate is assigned from the bottom to the top of lamina with z-axis upward. The properties associated with k^{th} layer in the laminate is designated k^{th} in the subscript of the property. Each ply strain can be calculated by using the following relationship:

$$\begin{bmatrix} \varepsilon_{\mathrm{x}} \\ \varepsilon_{\mathrm{y}} \\ \gamma_{\mathrm{xy}} \end{bmatrix}_{k^{th}} = \begin{bmatrix} \varepsilon_{\mathrm{x}}^{\mathrm{o}} \\ \varepsilon_{\mathrm{y}}^{\mathrm{o}} \\ \gamma_{\mathrm{xy}}^{\mathrm{o}} \end{bmatrix} + \mathrm{z}_{k^{th}} \begin{bmatrix} \kappa_{\mathrm{x}} \\ \kappa_{\mathrm{y}} \\ \kappa_{\mathrm{xy}} \end{bmatrix} \tag{2.15}$$

Where $\varepsilon_{\mathrm{x}}^{\mathrm{o}}$, $\varepsilon_{\mathrm{y}}^{\mathrm{o}}$ and $\gamma_{\mathrm{xy}}^{\mathrm{o}}$ are the mid-plane strains, κ_{x}, κ_{y} and κ_{xy} are the mid plane curvatures, z is the distance from mid-plane to any point of layer.

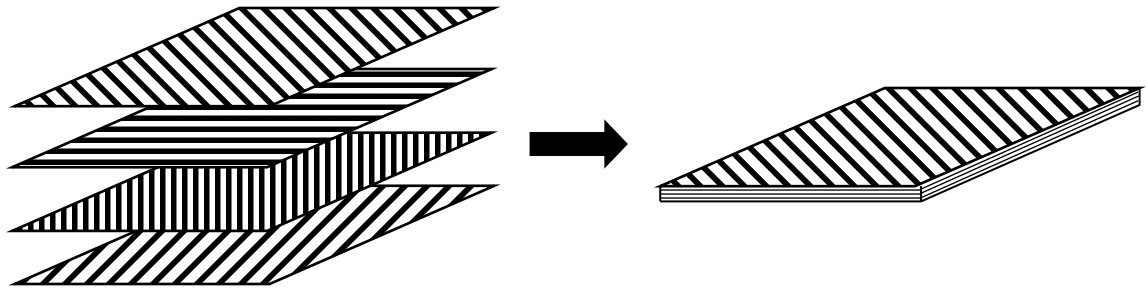

Figure 2.3 Several plies with different fiber orientation perfectly bonded together

Substituting equation (2.15) into equation (2.5), the stress of k^{th} ply can be expressed in term of mid-plane strains and curvatures as follows:

$$\begin{bmatrix}\sigma_x\\ \sigma_y\\ \tau_{xy}\end{bmatrix}_{kth} = [\overline{Q}]_{k^{th}}\begin{bmatrix}\varepsilon_x\\ \varepsilon_y\\ \gamma_{xy}\end{bmatrix}_{kth} = [\overline{Q}]_{k^{th}}\left\{\begin{bmatrix}\varepsilon_x^o\\ \varepsilon_y^o\\ \gamma_{xy}^o\end{bmatrix} + z_{k^{th}}\begin{bmatrix}\kappa_x\\ \kappa_y\\ \kappa_{xy}\end{bmatrix}\right\} \tag{2.16}$$

2.7 Constitutive Equation of Laminated Plate

The in-plane force [N] and moment [M] per unit width of laminate can be calculated by integrating force of each ply through the thickness of laminate:

$$\begin{bmatrix}N_x\\ N_y\\ N_{xy}\end{bmatrix} = \sum_{k=1}^{n}\int_{-h_{k-1}}^{h_k}\begin{bmatrix}\sigma_x\\ \sigma_y\\ \tau_{xy}\end{bmatrix}dz \tag{2.17}$$

$$\begin{bmatrix}M_x\\ M_y\\ M_{xy}\end{bmatrix} = \sum_{k=1}^{n}\int_{-h_{k-1}}^{h_k}\begin{bmatrix}\sigma_x\\ \sigma_y\\ \tau_{xy}\end{bmatrix}zdz \tag{2.18}$$

Where h_k is a distance from mid-plane to the upper surface of the k^{th} ply

Figure 2.4 illustrates loading components that act on the laminate.

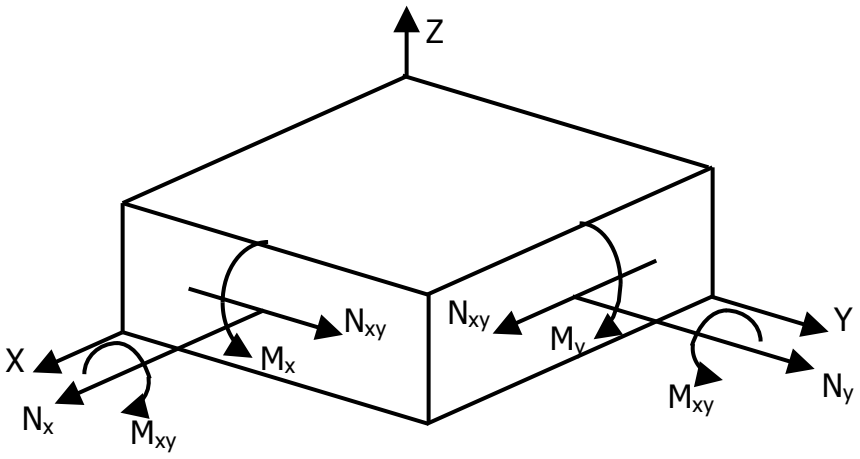

Figure 2.4 Loading components for in-plane laminate

Substituting equation (2.16) in equation (2.17 & 2.18), the constitutive equation of laminate can be expresses as follow:

$$\begin{bmatrix} N_x \\ N_y \\ N_{xy} \\ M_x \\ M_y \\ M_{xy} \end{bmatrix} = \begin{bmatrix} A_{11} & A_{12} & A_{16} & B_{11} & B_{12} & B_{16} \\ A_{21} & A_{22} & A_{26} & B_{12} & B_{22} & B_{26} \\ A_{16} & A_{26} & A_{66} & B_{16} & B_{26} & B_{66} \\ B_{11} & B_{12} & B_{16} & D_{11} & D_{12} & D_{16} \\ B_{12} & B_{22} & B_{26} & D_{21} & D_{22} & D_{26} \\ B_{16} & B_{26} & B_{66} & D_{16} & D_{26} & D_{66} \end{bmatrix} \begin{bmatrix} \varepsilon_x^o \\ \varepsilon_y^o \\ \gamma_{xy}^o \\ \kappa_x \\ \kappa_y \\ \kappa_{xy} \end{bmatrix} \text{ or } \begin{bmatrix} N \\ M \end{bmatrix} = \begin{bmatrix} A & B \\ B & D \end{bmatrix} \begin{bmatrix} \varepsilon^\circ \\ K \end{bmatrix} \quad (2.19)$$

Where [A] is in-plane extensional stiffness matrix, [B] is extensional-bending coupling stiffness matrix and [D] is the bending stiffness matrix. We can express the stiffness matrices [A], [B], and [D] as follow:

$$[A] = \sum_{k=1}^{n} [\overline{Q}]_k \cdot (h_k - h_{k-1}) \quad (2.20)$$

$$[B] = \frac{1}{2} \sum_{k=1}^{n} [\overline{Q}]_k \cdot (h_k^2 - h_{k-1}^2) \quad (2.21)$$

$$[D] = \frac{1}{3} \sum_{k=1}^{n} [\overline{Q}]_k \cdot (h_k^3 - h_{k-1}^3) \quad (2.22)$$

Where the subscript k indicates the layer number (Figure 2.5). It should be noted that [A], [B] and [D] matrices are symmetric matrices

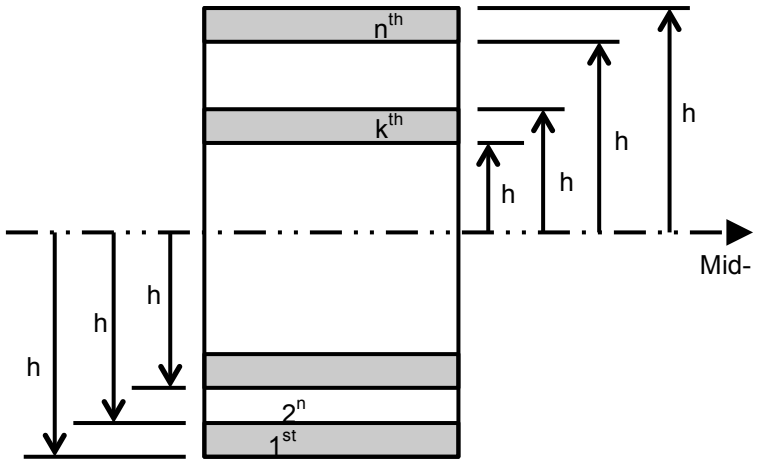

Figure 2.5 Geometry of an n-layer laminate

2.8 Narrow Beam VS Wide Beam

Figure 2.6 illustrates the defection of the narrow beam and wide beam. Narrow beam refers to the cross-section beam which the width-to-thickness ratio is small. There have induced lateral curvature due to Poison's effect [12], the lateral moment can be ignored ($\kappa_y \neq 0$, $M_y = 0$). While the wide beam has a large width-to-thickness ratio, the curvature occurred only on the edge of beam. Hence, there is no curvature on center area, so the induced lateral curvature is insignificant. The lateral moment need to be considered ($\kappa_y = 0$, $M_y \neq 0$).

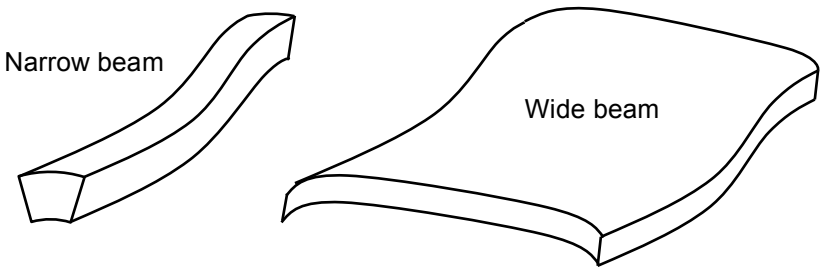

Figure 2.6 Narrow beam vs wide beam

For C-channel case, the beam is considered as narrow beam. The constitutive equation of narrow beam is written as below [8].

$$\begin{bmatrix} N_x \\ M_x \end{bmatrix} = \begin{bmatrix} A^* & B^* \\ B^* & D^* \end{bmatrix} \begin{bmatrix} \varepsilon_x^0 \\ \kappa_x \end{bmatrix} \text{ or } \begin{bmatrix} \varepsilon_x^0 \\ \kappa_x \end{bmatrix} = \begin{bmatrix} a^* & b^* \\ b^* & d^* \end{bmatrix} \begin{bmatrix} N_x \\ M_x \end{bmatrix} \quad (2.23)$$

Where

$$a^* = a_{11} - b_{16}^2 / d_{66} \qquad b^* = b_{11} - b_{16} d_{16} / d_{66} \qquad d^* = d_{11} - d_{16}^2 / d_{66} \quad (2.24)$$

CHAPTER 3

ANALYTICAL METHOD FOR COMPOSITE LAMINATED WITH C-CHANNEL CROSS-SECTION

3.1 Geometric of Composite Laminate with C-channel

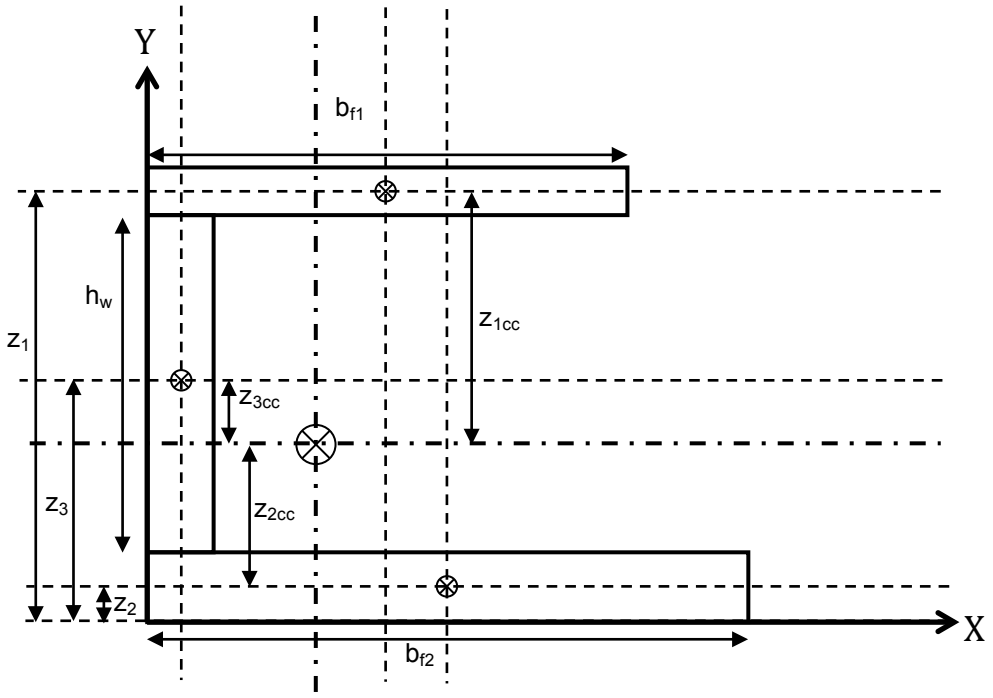

Figure 3.1 Geometry of composite beam with C-Channel cross-section

The geometry of composite C-Channel is shown in figure 3.1. There can be divided into three sections that compose of three sub-laminates top flange, bottom flange, and web.

Where b_{f1}, b_{f2}, and h_w are width of top flange, bottom flange and web, respectively. z_1, z_2, and z_3 are distance from Y-axis to centroid of top flange, bottom flange and web, respectively.

3.2 Centroid of Composite Laminate with C-Channel

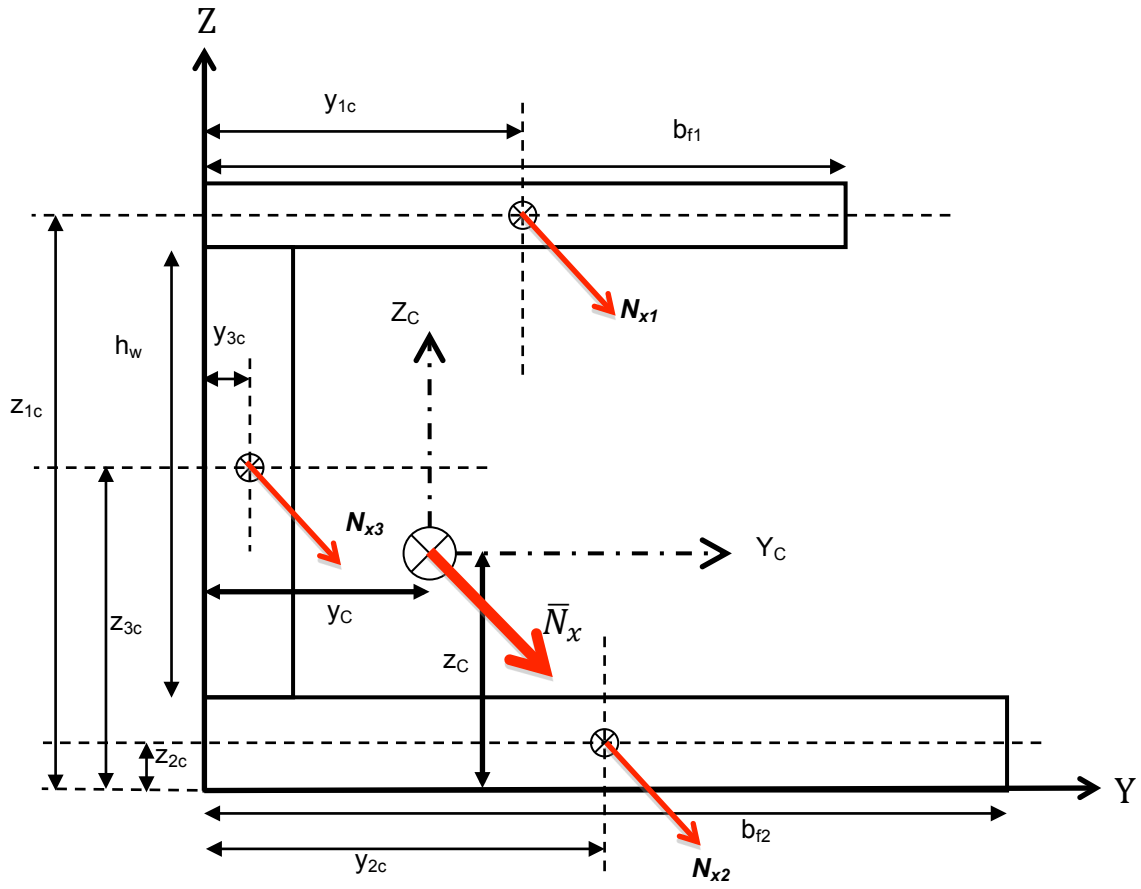

Figure 3.2 Axial forces on centroid of each sub-laminate

The centroid of cross-section is the location of average force acting, at the centroid, an axial load ($\bar{N}_x$) doesn't induced curvature (κ_x^c & κ_z^c), and bending moments ($\bar{M}_x$ & $\bar{M}_z$) don't produce axial strain (ε_x^c). To calculate centroid, set Y-axis at the most bottom of the bottom flange and Z-axis at the most left of web as shown in figure 3.2. Apply axial force on the centroid of each laminate. The total force will be acting on the centroid.

The total moment and total axial force for Y-axis are given as::

$$\bar{N}_x z_c = N_{x1} b_{f1} z_{1c} + N_{x2} b_{f2} z_{2c} + N_{x3} h_w z_{3c} \tag{3.1}$$

$$\overline{N}_x = N_{x1}b_{f1} + N_{x2}b_{f2} + N_{x3}h_w \tag{3.2}$$

Then, we have

$$z_c = \frac{N_{x1}b_{f1}z_{1c}+N_{x2}b_{f2}z_{2c}+N_{x3}b_w z_{3c}}{N_{x1}b_{f1}+N_{x2}b_{f2}+N_{x3}b_w} \tag{3.3}$$

Appling constitutive equation for narrow laminate beam (equation (2.23) & (2.24)), so equation (3.3) can be modified as:

$$z_c = \frac{A^*_{f1}b_{f1}z_{1c}+A^*_{f2}b_{f2}z_{2c}+A^*_w b_w z_{3c}}{A^*_{f1}b_{f1}+A^*_{f2}b_{f2}+A^*_w b_w} \tag{3.4}$$

It is noted that the subscripts, f and w in A*, B* and D* refer to the flange and web laminates, respectively.

Similarly, Centroid in Z-axis can be calculates by the same procedure and gets the result as follow:

$$y_c = \frac{A^*_{f1}b_{f1}y_{1c}+A^*_{f2}b_{f2}y_{2c}+A^*_w b_w y_{3c}}{A^*_{f1}b_{f1}+A^*_{f2}b_{f2}+A^*_w b_w} \tag{3.5}$$

3.3 Equivalent Stiffness

The stiffness is the rigidity of the material which resists the deformation under an applied force. There are three types of stiffnesses, axial, bending and torsion stiffness. This research focuses on axial and bending stiffnesses.

The axial and bending stiffnesses are used for predicting the response of structure under load. To evaluate the equivalent stiffnesses, axial force & bi-axial bending moment are applied at the centroid of cross-section, the load components were shown on figure 3.3. The governing equation will be writing as:

$$\begin{bmatrix} \overline{N}_x \\ \overline{M}_x \\ \overline{M}_z \end{bmatrix} = \begin{bmatrix} \overline{EA} & 0 & 0 \\ 0 & \overline{D}_x & \overline{D}_{xy} \\ 0 & \overline{D}_{xy} & \overline{D}_y \end{bmatrix} \begin{bmatrix} \varepsilon_x^c \\ \kappa_x^c \\ \kappa_z^c \end{bmatrix} \tag{3.6}$$

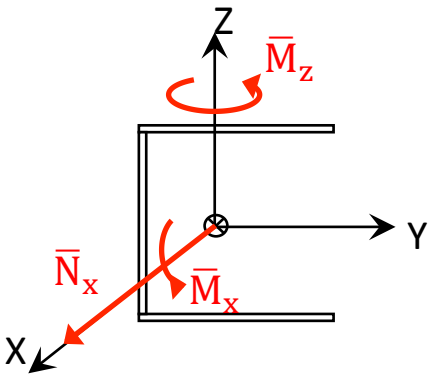

Figure 3.3 Loads component

The beam is subject to a bi-axial bending then the mid-plane strain can be written in term of centroid strain and bi-axial curvature as following:

$$\varepsilon_x^o = \varepsilon_x^c + z\kappa_x^c + y\kappa_z^c \tag{3.7}$$

3.3.1 Axial Stiffness

The axial stiffness can be considered as the resistance of the structure to deform along axial load.

Let assume the total axial force and all three sub-laminates' axial force were applied at the centroid of the C-channel cross-section and each sub-laminate, respectively.

From the 1st equation of equation (3.6) can be writing as

$$\bar{N}_x = \overline{EA}\varepsilon_x^c \tag{3.8}$$

The summation of sub-laminates' axial force equal to total axial force

$$\bar{N}_x = b_{f1}\bar{N}_{x,f1} + b_{f2}\bar{N}_{x,f2} + h_w\bar{N}_{x,w} \tag{3.9}$$

From constitutive equation of narrow beam;

$$\bar{N}_x = b_{f1}(A_{f1}^*\varepsilon_{x,f1}^o + B_{f1}^*\kappa_{x,f1}) + b_{f2}(A_{f2}^*\varepsilon_{x,f2}^o + B_{f2}^*\kappa_{x,f2}) + h_w(A_w^*\varepsilon_{x,w}^o) \tag{3.10}$$

The strains for all laminates are equal the total strain along the x-axis and there have no curvature for all laminates due to load at the centroid of the entire cross-section. The constitutive equation can be rewrite as:

$$\overline{N}_x = \{A^*_{f1}b_{f1} + A^*_{f2}b_{f2} + A^*_w h_w\}\varepsilon^c_x \tag{3.11}$$

Comparing equation (3.11) with equation (3.8), axial stiffness can be writing as:

$$\overline{EA} = A^*_{f1}b_{f1} + A^*_{f2}b_{f2} + A^*_w h_w \tag{3.12}$$

3.3.2 Bending Stiffness

To evaluate$\overline{D}_x$, from the 2nd equation of equation (3.6), only moment in x-direction ($\overline{M}_x$) was applied. The curvature κ^c_z can be suppressed;

$$\overline{M}_x = \overline{D}_x \kappa^c_x \tag{3.13}$$

$$\overline{M}_x = b_{f1}(N_{x1}z_{1cc} + M_{x1}) + b_{f2}(N_{x2}z_{2cc} + M_{x2}) + \left\{\int_{-\left(\frac{h_w}{2} - z_{3cc}\right)}^{\left(\frac{h_w}{2} + z_{3cc}\right)} zN_{x3}dz\right\} \tag{3.14}$$

From equation (3.14), consider sub-laminate 1 (top flange), Then using constitutive equation for narrow beam, we obtain

$$b_{f1}(N_{x1}z_{1cc} + M_{x1}) = b_{f1}\left\{\left(A^*_{f1}\varepsilon^o_{x,f1} + B^*_{f1}\kappa_{x,f1}\right)z_{1cc} + \left(B^*_{f1}\varepsilon^o_{x,f1} + D^*_{f1}\kappa_{x,f1}\right)\right\} \tag{3.15}$$

The mid-plane strain can be obtained by CLT as, $\varepsilon^o_{x,f1} = \varepsilon^c_x + z_{1cc}\kappa^c_x + y_{1cc}\kappa^c_z$, but there have no strain at centroid ($\varepsilon^c_x = 0$) and curvature about z-direction was suppressed ($\kappa^c_z = 0$). Curvatures about x-direction at any point are the same as curvature at the centroid, $\kappa_{x,f1} = \kappa^c_x$. The equation (3.15) can be modified as follow;

$$b_{f1}(N_{x1}z_{1cc} + M_{x1}) = b_{f1}(A^*_{f1}z^2_{1cc} + 2B^*_{f1}z_{1cc} + D^*_{f1})\kappa^c_x \tag{3.16}$$

Where z_{1mc} is the distance from mid-plane of the top flange to the cross-section centroid.

For, sub-laminate 2 (bottom flange), we have;

$$b_{f2}(N_{x2}z_{2cc} + M_{x2}) = b_{f2}(A^*_{f2}z^2_{1cc} + 2B^*_{f1}z_{1cc} + D^*_{f1})\kappa^c_x \tag{3.17}$$

For sub-laminate 3 (web), the integral become

$$\int_{-\left(\frac{h_w}{2}-z_{3cc}\right)}^{\left(\frac{h_w}{2}+z_{3cc}\right)} zN_{x3}dz \;= A^*_w\left\{\frac{h^3_w}{12} + h_w z^2_{3cc}\right\}\kappa^c_x \tag{3.18}$$

Substitute equation (3.16) to equation (3.18) into equation (3.14)

$$\overline{M}_x = \left[b_{f1}(A^*_{f1}z^2_{1cc} + 2B^*_{f1}z_{1cc} + D^*_{f1}) + b_{f2}(A^*_{f2}z^2_{2cc} + 2B^*_{f2}z_{2cc} + D^*_{f2}) + A^*_w\left(\frac{h^3_w}{12} + h_w z^2_{3cc}\right)\right]\kappa^c_x \tag{3.19}$$

Comparing equation (3.19) with equation (3.16), bending stiffness can be written as:

$$\overline{D}_x = \left[b_{f1}(A^*_{f1}z^2_{1cc} + 2B^*_{f1}z_{1cc} + D^*_{f1}) + b_{f2}(A^*_{f2}z^2_{2cc} + 2B^*_{f2}z_{2cc} + D^*_{f2}) + A^*_w\left(\frac{h^3_w}{12} + h_w z^2_{3cc}\right)\right] \tag{3.20}$$

To obtain the bending stiffness, $\overline{D}_y$, we apply $\overline{M}_z$ at the centroid. Hence we have;

$$\overline{M}_z = \overline{D}_y\kappa^c_z \tag{3.21}$$

$$\overline{M}_z = \left\{\int_{-\left(\frac{b_{f1}}{2}-y_{1cc}\right)}^{\left(\frac{b_{f1}}{2}+y_{1cc}\right)} yN_{x1}dy\right\} + \left\{\int_{-\left(\frac{b_{f2}}{2}-y_{2cc}\right)}^{\left(\frac{b_{f2}}{2}+y_{2cc}\right)} yN_{x2}dy\right\} + \{N_{x3}h_w y_{3cc} + M_{x1}h_w\} \tag{3.22}$$

To evaluate bending stiffness, $\overline{D}_y$, the same procedure used for $\overline{D}_x$ is introduced. Then the result can be obtained as follow;

$$\overline{D}_y = A^*_{f1}\left\{\frac{b^3_{f1}}{12} + b_{f1}y^2_{1cc}\right\} + A^*_{f2}\left\{\frac{b^3_{f2}}{12} + b_{f2}y^2_{2cc}\right\} + \{A^*_w y^2_{3cc} + 2B^*_w y_{3cc} + D^*_w\} \tag{3.23}$$

To calculate $\overline{D}_{xy}$, use the the 2nd equation, to obtain the bending stiffness, $\overline{D}_{xy}$, apply $\overline{M}_x$. The curvature κ_x^c is suppressed.

$$\overline{M}_x = \overline{D}_{xy}\kappa_z^c \tag{3.24}$$

From equation (3.14), consider sub-laminate 1 (top flange), sub-laminate 2 (bottom flange) and sub-laminate 3 (Web). The mid-plane strain can be obtained by lamination theory as, $\varepsilon_{x,f1}^o = \varepsilon_x^c + y_{1mc}\kappa_z^c$, but $\varepsilon_z^c = 0$ because no strain at centroid. Curvatures at any point are the same as curvature at the centroid, $\kappa_{x,f1} = \kappa_z^c$.

$$b_{f1}(N_{x1}z_{1cc} + M_{x1}) = b_{f1}(A_{f1}^*z_{1cc} + B_{f1}^*)y_{1cc}\kappa_z^c \tag{3.25}$$

$$b_{f2}(N_{x2}z_{2cc} + M_{x2}) = b_{f2}(A_{f2}^*z_{2cc} + B_{f2}^*)y_{2cc}\kappa_z^c \tag{3.26}$$

$$\int_{-\left(\frac{h_w}{2}-z_{3cc}\right)}^{\left(\frac{h_w}{2}+z_{3cc}\right)} zN_{x3}dz \;= (A_w^*y_{3cc} + B_w^*)h_w z_{3cc}\kappa_z^c \tag{3.27}$$

Substituting equation (3.25), (3.26) and (3.27) into equation (3.14), the bending stiffness can be written as:

$$\overline{D}_{xy} = (A_{f1}^*z_{1cc} + B_{f1}^*)b_{f1}y_{1cc} + (A_{f2}^*z_{2cc} + B_{f2}^*)b_{f2}y_{2cc} + (A_w^*y_{3cc} + B_w^*)h_w z_{3cc} \tag{3.28}$$

3.4 Ply Stress Analysis

The strain and curvature at the centroid of each laminated are calculated. There is the point where no axial-bending stiffness coupling. ε_x^c, κ_x^c and κ_z^c can be obtaining by modifies three equations in equation (3.6) follow:

$$\varepsilon_x^c = \frac{\overline{N}_x}{\overline{E}\overline{A}} \tag{3.29}$$

$$\kappa_x^c = \frac{\overline{M}_x\overline{D}_y - \overline{M}_z\overline{D}_{xy}}{\overline{D}_x\overline{D}_y - \overline{D}_{xy}^2} \tag{3.30}$$

$$\kappa_z^c = \frac{\bar{M}_z\bar{D}_x - \bar{M}_x\bar{D}_{xy}}{\bar{D}_x\bar{D}_y - \bar{D}_{xy}^2} \tag{3.31}$$

3.4.1 Top Flange (sub-laminate 1)

From constitutive equation for narrow beam, axial force and bending moment on the top flange can be expressed as:

$$N_{x,f1} = A^*\varepsilon_{x,f1}^0 + B^*\kappa_{x,f1} \tag{3.32}$$

$$M_{x,f1} = B^*\varepsilon_{x,f1}^0 + D^*\kappa_{x,f1} \tag{3.33}$$

Where $\varepsilon_{x,f1}^0 = \varepsilon_x^c + z_{1mc}\kappa_x^c + y_1\kappa_z^c$ and $\kappa_{x,f1} = \kappa_x^c$

z_{1mc} : distance from centroid to mid-plane of top flange

y_1 : distance from centroid to any point of top flange

Equation (3.29) and equation (3.31) become:

$$N_{x,f1} = A^*(\varepsilon_x^c + z_{1mc}\kappa_x^c + y_1\kappa_z^c) + B^*\kappa_x^c \tag{3.34}$$

$$M_{x,f1} = B^*(\varepsilon_x^c + z_{1mc}\kappa_x^c + y_1\kappa_z^c) + D^*\kappa_x^c \tag{3.35}$$

The mid-plane strains and curvature of top flange are

$$\begin{bmatrix} \varepsilon_x^0 \\ \varepsilon_y^0 \\ \gamma_{xy}^0 \\ \kappa_x \\ \kappa_y \\ \kappa_{xy} \end{bmatrix}_{f1} = \begin{bmatrix} a_{11} & b_{11} & b_{16} \\ a_{12} & b_{12} & b_{26} \\ a_{16} & b_{16} & b_{66} \\ b_{11} & d_{11} & d_{16} \\ b_{12} & d_{12} & d_{26} \\ b_{16} & d_{16} & d_{66} \end{bmatrix}_{f1} \begin{bmatrix} N_{x,f1} \\ M_{x,f1} \\ M_{xy,f1} \end{bmatrix} \tag{3.36}$$

From the 6th equation: $\kappa_{xy,f1} = b_{16}N_{x,f1} + d_{16}M_{x,f1} + d_{66}M_{xy,f1} = 0$

$$M_{xy,f1} = -\frac{(b_{16,f1}N_{x,f1} + d_{16,f1}M_{x,f1})}{d_{66,f1}} \tag{3.37}$$

From equation (3.36) and equation (3.37) we can calculate ε_x^0, ε_y^0, γ_{xy}^0, κ_x and κ_y

$$\varepsilon_x^0 = \left(a_{11} - \frac{b_{16}^2}{d_{66}}\right)_{f1} N_{x,f1} + \left(b_{11} - \frac{b_{16}d_{16}}{d_{66}}\right)_{f1} M_{x,f1} \tag{3.38}$$

$$\varepsilon_y^0 = \left(a_{12} - \frac{b_{16}b_{26}}{d_{66}}\right)_{f1} N_{x,f1} + \left(b_{12} - \frac{b_{26}d_{16}}{d_{66}}\right)_{f1} M_{x,f1} \tag{3.39}$$

$$\gamma_{xy}^0 = \left(a_{16} - \frac{b_{16}b_{66}}{d_{66}}\right)_{f1} N_{x,f1} + \left(b_{16} - \frac{b_{66}d_{16}}{d_{66}}\right)_{f1} M_{x,f1} \tag{3.40}$$

$$\kappa_x = \left(b_{11} - \frac{b_{16}d_{16}}{d_{66}}\right)_{f1} N_{x,f1} + \left(d_{11} - \frac{d_{16}^2}{d_{66}}\right)_{f1} M_{x,f1} \tag{3.41}$$

$$\kappa_y = \left(b_{12} - \frac{b_{16}d_{26}}{d_{66}}\right)_{f1} N_{x,f1} + \left(d_{12} - \frac{d_{16}d_{26}}{d_{66}}\right)_{f1} M_{x,f1} \tag{3.42}$$

We can calculate strain of each ply by classical lamination theory. Equation (2.15) can be modified as;

$$\begin{bmatrix}\varepsilon_x \\ \varepsilon_y \\ \gamma_{xy}\end{bmatrix}_{k^{th},f1} = \begin{bmatrix}\varepsilon_x^0 \\ \varepsilon_y^0 \\ \gamma_{xy}^0\end{bmatrix}_{f1} + z_{k^{th},f1}\begin{bmatrix}\kappa_x \\ \kappa_y \\ 0\end{bmatrix}_{f1} \tag{3.43}$$

From k^{th} ply strain, we can determine stress on each ply.

$$\begin{bmatrix}\sigma_x \\ \sigma_y \\ \tau_{xy}\end{bmatrix}_{k^{th},f1} = [\bar{Q}]_{k^{th},f1}\left\{\begin{bmatrix}\varepsilon_x^0 \\ \varepsilon_y^0 \\ \gamma_{xy}^0\end{bmatrix}_{f1} + z_{k^{th},f1}\begin{bmatrix}\kappa_x \\ \kappa_y \\ 0\end{bmatrix}_{f1}\right\} \tag{3.44}$$

3.4.2 Bottom Flange (sub-laminate 2)

To calculate the bottom flange used the same procedure as for the top flange, we have

$$\begin{bmatrix}\sigma_x \\ \sigma_y \\ \tau_{xy}\end{bmatrix}_{k^{th},f2} = [\bar{Q}]_{k^{th},f2}\left\{\begin{bmatrix}\varepsilon_x^0 \\ \varepsilon_y^0 \\ \gamma_{xy}^0\end{bmatrix}_{f2} + z_{k^{th},f2}\begin{bmatrix}\kappa_x \\ \kappa_y \\ 0\end{bmatrix}_{f2}\right\} \tag{3.45}$$

3.4.3 Web (sub-laminate 3)

The procedure same as top flange, but the constitutive equation for narrow beam of the sub-laminate loads can be express as in term of curvature about z-axis, $\kappa_{z,w}$.

$$N_{x,w} = A^*\varepsilon^0_{x,w} + B^*\kappa_{z,w} \tag{3.46}$$

$$M_{x,w} = B^*\varepsilon^0_{x,w} + D^*\kappa_{z,w} \tag{3.47}$$

Where $\varepsilon^0_{x,f1} = \varepsilon^c_x + z_3\kappa^c_x + y_{3mc}\kappa^c_z$ and $\kappa_{x,w} = \kappa^c_z$

$$N_{x,f1} = A^*(\varepsilon^c_x + z_3\kappa^c_x + y_{3mc}\kappa^c_z) + B^*\kappa^c_z \tag{3.48}$$

$$M_{x,f1} = B^*(\varepsilon^c_x + z_3\kappa^c_x + y_{3mc}\kappa^c_z) + D^*\kappa^c_z \tag{3.49}$$

z_3 : distance from centroid to any point of web

y_{3mc} : distance from centroid to mid-plane of web

The procedure to calculate the mid-plane strains and curvature, the strain and stress of each k^{th} ply of the web is the same as used in the flange. But consider distance in y-axis instead of z-axis. The stress of k^{th} ply can be expressed as;

$$\begin{bmatrix}\sigma_x\\ \sigma_y\\ \tau_{xy}\end{bmatrix}_{k^{th},w} = [\overline{Q}]_{k^{th},w}\left\{\begin{bmatrix}\varepsilon^0_x\\ \varepsilon^0_y\\ \gamma^0_{xy}\end{bmatrix}_w + y_{k^{th},w}\begin{bmatrix}\kappa_x\\ \kappa_y\\ \kappa_{xy}\end{bmatrix}_w\right\} \tag{3.50}$$

3.5 Flow Chart of Composite Procedures

The overall computation procedure is depicted in Figure 3.4. After obtaining the ply stresses, failure criteria can be applied for conducting the ply failure analysis, which is not in the scope of this study.

Figure 3.4 Computation Procedure of the Stress Analysis for C-channel beam

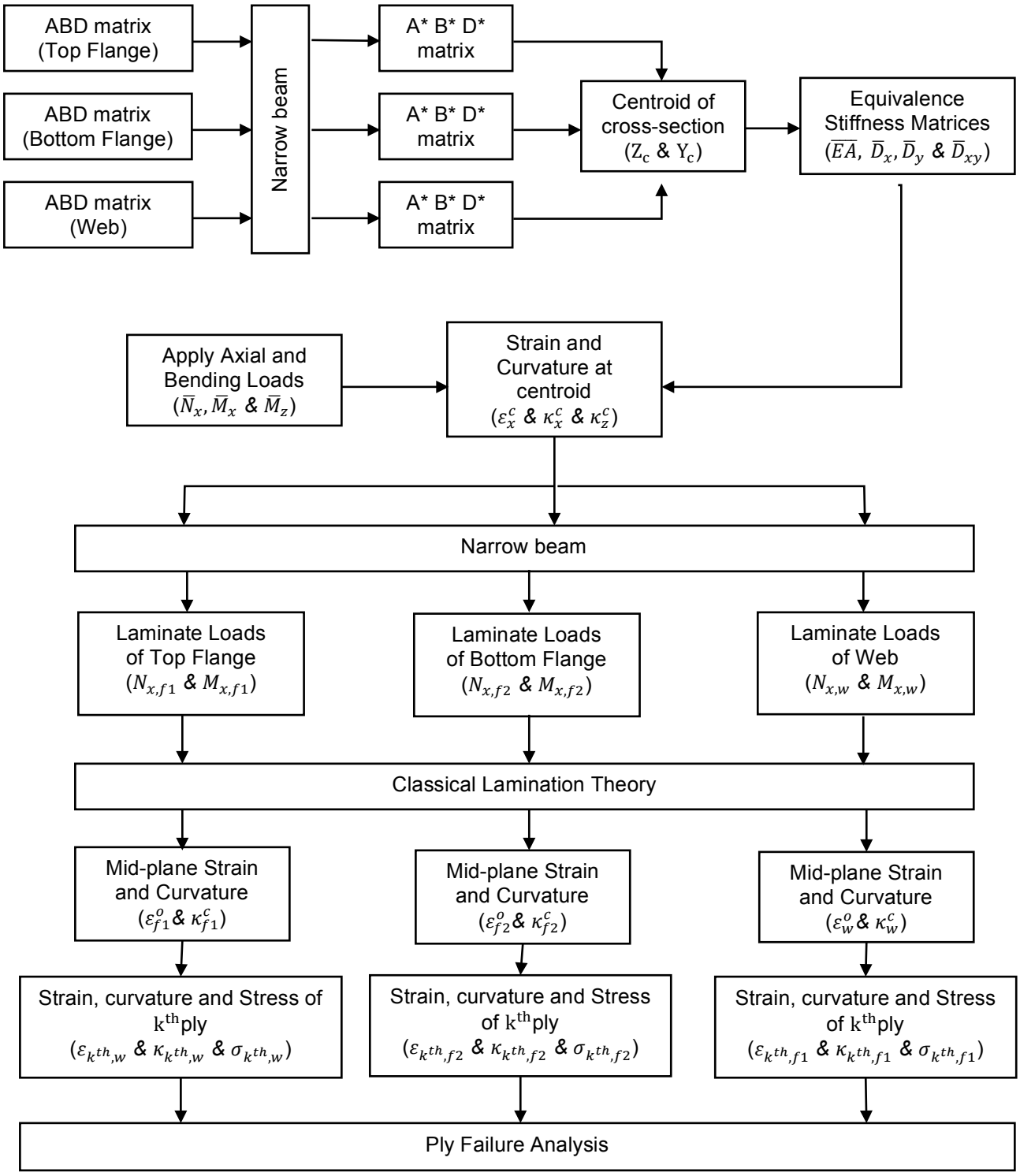

CHAPTER 4

FINITE ELEMENT METHOD

In this chapter refers to the modeling and analysis of composite laminated C-Channel with Finite Element Method using ANSYS 13.0. This program was designed for solving several of mechanical problems that include static/dynamic structure analysis, heat transfer and fluid problems. This chapter also gives the detail of geometry, material properties, and laminate configuration.

Analysis ply stress of composite laminated C-Channel is a major purpose of this research. In general, to do analysis by ANSYS can be mainly dividing into three stages, modeling, solving and post processing.

4.1 Modeling

4.1.1 Geometry of Composite Laminate

This stage is described how to create the 3D model of C-Channel of composite laminated beam. The model uses SHELL181 element, a two-dimension shell element with 4 nodes with 6 degrees of freedom at each node, because this element is suitable for thin to moderately thick shell structure. Each laminate was treated as area element, formed by 4 nodes.

To modeling the three-dimension model, 8 keypoints were defined as main structure C-Channel shape and 1 keypoint was defined as centroid of cross-section. The length of model is 10 inches. Figure 4.1 shows that three areas were created base on 8 keypoints; A1 is the top flange, A2 is the bottom flange and A3 is the web. The width of each laminate (location of keypoints) can be subject to change for other geometry problem.

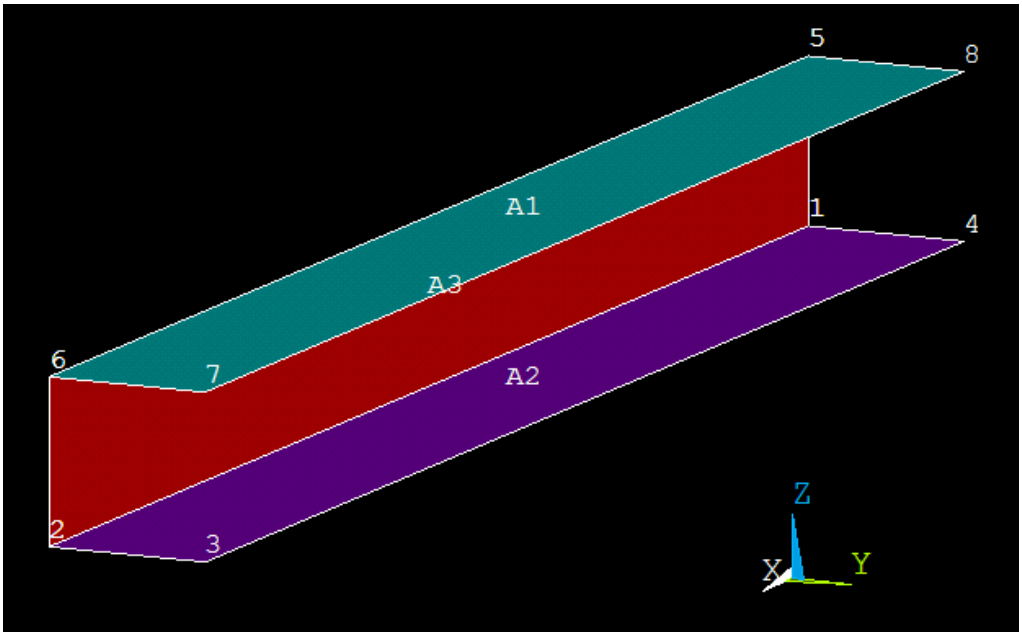

Figure 4.1 Geometry of C-channel beam

4.1.2 Material Properties

The material used for composite laminate is AS/3501 graphite/epoxy. The material properties as shown below:

$E_1 = 20.00 \times 10^6$ psi $E_2 = 1.3 \times 10^6$ psi $E_3 = 1.3 \times 10^6$ psi

$V_{12} = 0.30$ $V_{13} = 0.30$ $V_{23} = 0.49$

$G_{12} = 1.03 \times 10^6$ psi $G_{13} = 1.03 \times 10^6$ psi $G_{23} = 0.90 \times 10^6$ psi

Where E_1, E_2, and E_3 are elastic moduli along fiber, transverse and perpendicular direction, respectively,

4.1.3 Laminated Configuration

The properties of element of SHELL181 can be set by input number of ply, fiber orientation and layer thickness. All three laminated were defined the shell element and shell configuration. The lay-up sequence of each laminate shown in Figure 4.2 was set up for [45/-45/0/90]s. The lowest ply can be set as first ply and the highest is the last ply.

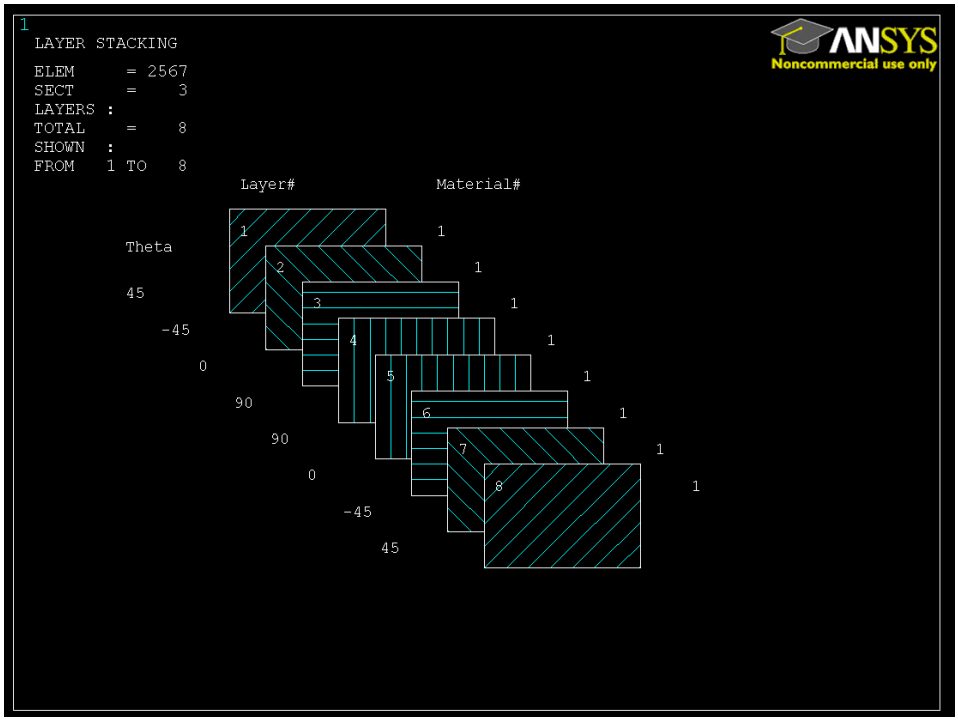

Figure 4.2 Laminated with stacking sequence of [45/-45/0/90]s

The shell configuration set for top flange, the #1 ply or the most bottom ply is inside the model and the last ply or the most top ply is outside the model. Bottom flange, the #1 ply or the most bottom ply is outside the model and the last ply or the most top ply is inside the model. Web, the #1 ply or the most left ply is outside the model and the last ply or the most right ply is inside the model. Figure 4.3 shows the set of each sub-laminate configuration.

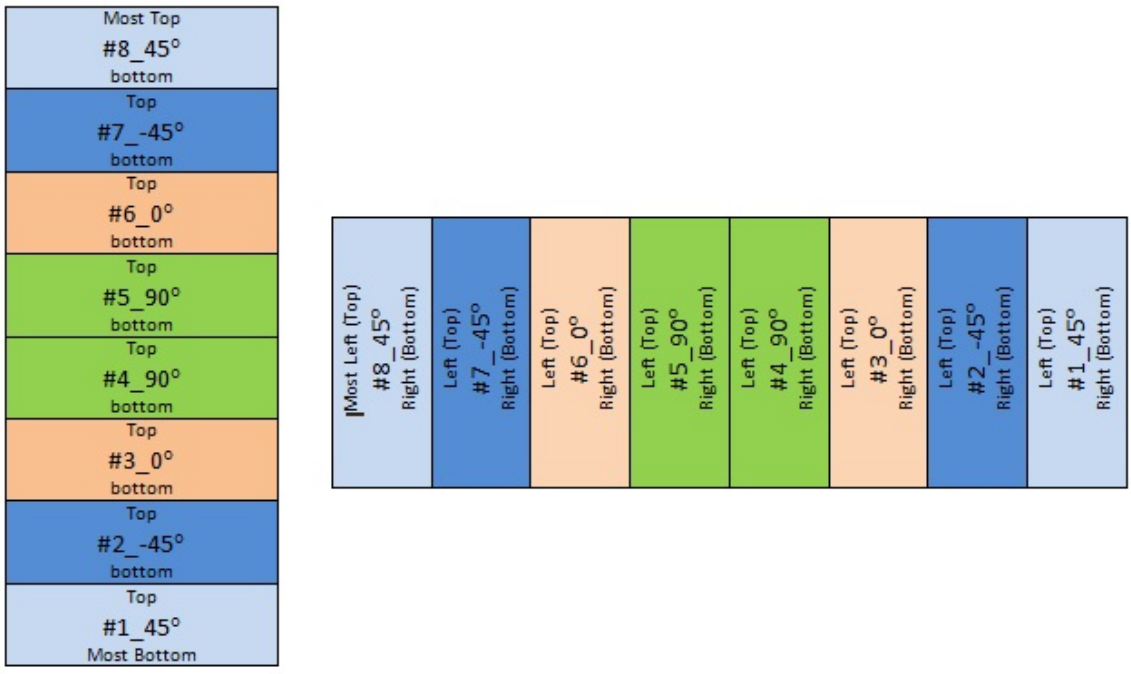

(a) (b)

Figure 4.3 Laminate configuration (a) top flange and bottom flange (b) web

4.1.4 Mashing

In this stage, the areas were mapped meshing. Each laminate was divided into width x 10 pieces along width direction and 100 pieces along the length (X-direction). In first case, width of all laminated are 1 in, so each laminated divided into 10 pieces as show in Figure 4.4. For another geometry, also depend on the width of each sub-laminated.

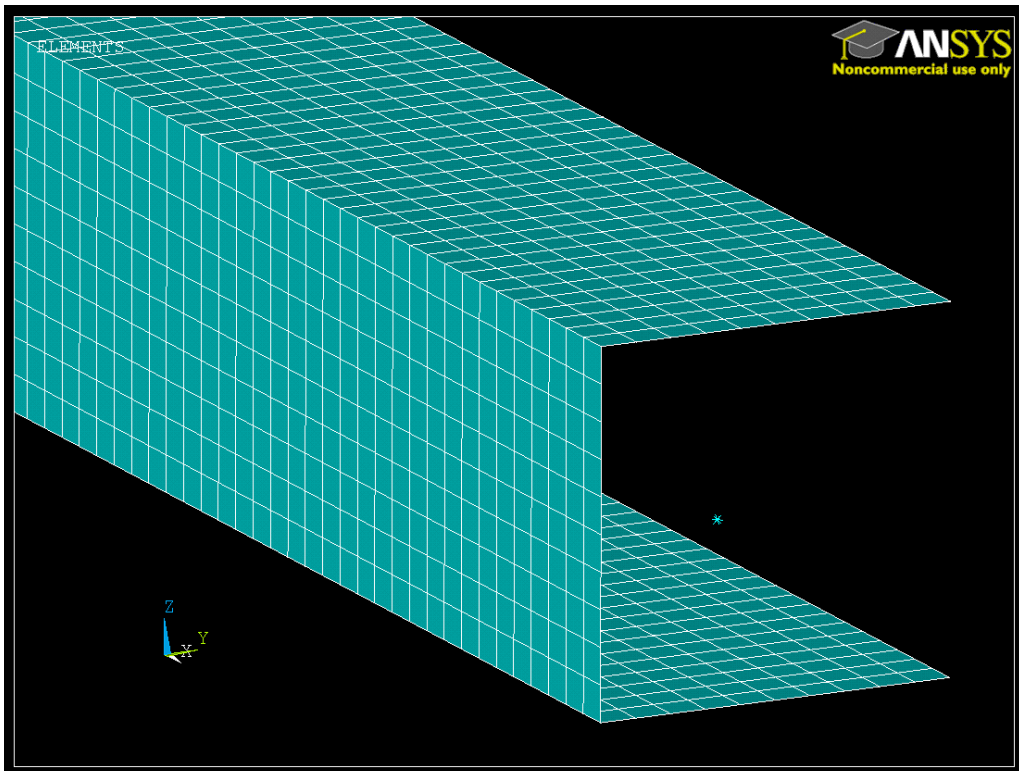

Figure 4.4 Mapped meshing of model

4.2 Solving

After the model ready, there have to set condition of the model before loads and constrain were applied on the model.

For an axial load case, the normal force was applied at the centroid of the cross-section at one end while the other end is fixed. The location of centroid is out of model, all nodes at the end need to fix with centroid, so the MASS21 element was introduced.

Figure 4.5 shows axial force applied at the centroid of C-channel cross-section. The MASS21 was used as cross-section element to rigid every nodes at the end of beam along the cross-section to ensure that there have no defection on cross-section. For other cases that involved with centroid always use this process to apply load.

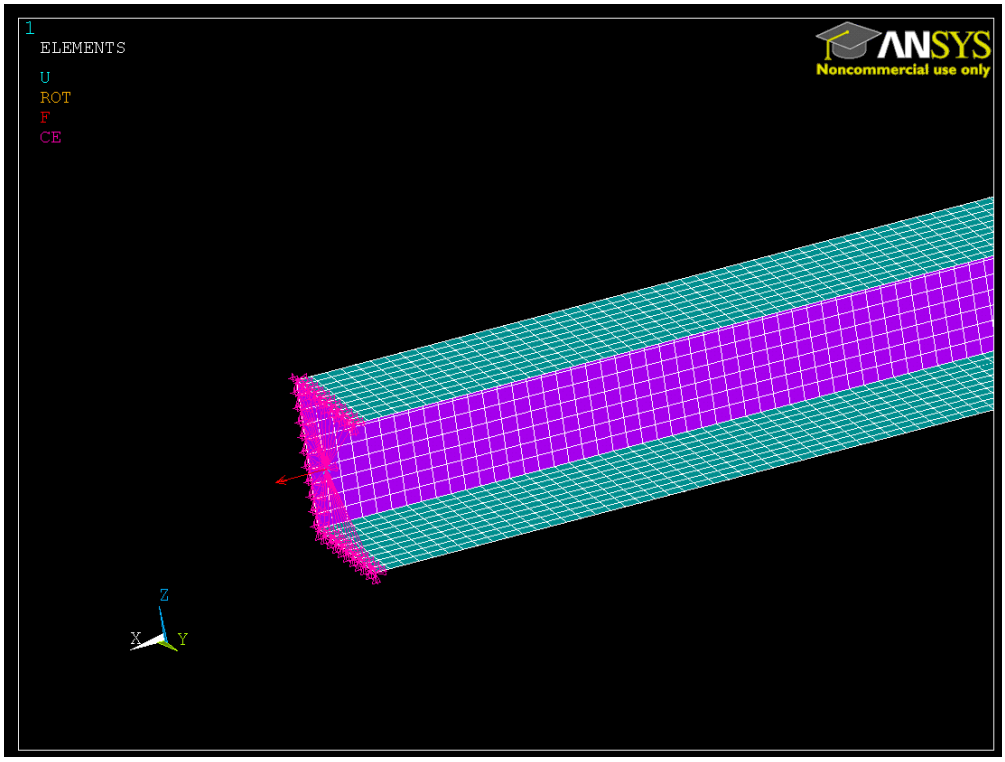

Figure 4.5 Axial load at the centroid of cross-section

4.3 Post Processing

This section deals with the result obtaining from ANSYS. The outputs were read via node solutions that were generated in the mashing process. The outputs that use as the results were measured at the mid length of beam. The measurement uses mid length cross-section because to prevent the deflection or effect of constrain and apply load at the ends of the beam.

For any case, nodes used to measure are at the mid-point of each laminate.

CHAPTER 5

RESULTS FOR LAMINATED COMPOSITE WITH C-CHANNEL

This chapter provides the solution from analytical solution that are derived in chapter 3. The cross-section properties and the ply stresses are calculated using the equations. These results then compared with the results obtained from FEM. There have 5 cases on this study

Case 1: Isotropic Material

- Material use is aluminum
- The width of all sub-laminates are one inch

Case 2: Composite Material with all laminate layup are $[0°]_{8T}$

- Material use is AS/3501 graphite/epoxy
- The width of all sub-laminates are one inch
- The stacking sequence of all sub-laminates are $[0°]_{8T}$

Case 3: Composite Material with all laminate layup are [±45°/0°/90°]s

- Material use is AS/3501 graphite/epoxy
- The width of all sub-laminates are one inch
- The stacking sequence of all sub-laminates are [±45°/0°/90°]s

Case 4: Composite Material with all laminate layup are [±45°/0°/90°]s and two-inch width of bottom flange

- Material use is AS/3501 graphite/epoxy
- The width of top flange and web are one inch
- The width of bottom flange is two inches
- The stacking sequence of all sub-laminates are [±45°/0°/90°]s

Case 5: Composite Material with unsymmetrical layup

- Material use is AS/3501 graphite/epoxy
- The width of all sub-laminates are one inch
- The stacking sequence of top flange and web are

  $[0/45/-45/90/45/0/-45/90]_T$
- The stacking sequence of bottom flange is

  $[90/-45/0/45/90/-45/45/0]_T$

The isotropic material was conducted to verify the present method. Table 5.1 summaries the dimension and layups of the laminates for all the five cases

Table 5.1 Case studies of C-channel laminate layups and dimensions

Case	Top Flange	Bottom Flange	Web
	Layup	Layup	Layup
	Dimension (in)	Dimension (in)	Dimension (in)
1	Aluminum	Aluminum	Aluminum
	1	1	1
2	$[0°]_{8T}$	$[0°]_{8T}$	$[0°]_{8T}$
	1	1	1
3	[±45°/0°/90°]s	[±45°/0°/90°]s	[±45°/0°/90°]s
	1	1	1
4	[±45°/0°/90°]s	[±45°/0°/90°]s	[±45°/0°/90°]s
	1	2	1
5	$[0/45/-45/90/45/0/-45/90]_T$	$[90/-45/0/45/90/-45/45/0]_T$	$[0/45/-45/90/45/0/-45/90]_T$
	1	1	1

5.1 Results of centroid of C-channel cross-section

5.1.1 Isotropic Material

The material for isotropic is aluminum, the material properties are follow;

E = 10.6 x 10^6 psi V = 0.33 G = 3.985 x 10^6 psi

For isotropic material, the centroid depends only on the geometric parameters. The centroid of C-beam with isotropic material can be obtained as;

$$z_c = \frac{\sum_i^n A_i z_i}{\sum_i^n A_i} \tag{5.1}$$

$$y_c = \frac{\sum_i^n A_i y_i}{\sum_i^n A_i} \tag{5.2}$$

Where n is number of division of area used to represent the C-channel. The centroid obtained from both methods shows an excellent agreement.

5.1.2 Composite Material

For composite material, there have no mechanics approach to calculate centroid. The centroid of composite laminate depends on the laminate configuration and fiber orientation. Compare with the same geometry between isotropic material and composite material with symmetrical and unsymmetrical laminate.

The material for composite is AS/3501 graphite/epoxy. The material properties already shown in chapter 4

Table 5.2 Result for centroid of C-channel for composite material

Case		unit	Present Method (Eq. 3.8 & 3.9)
2	Z_C	in	0.54
	Y_C	in	0.34
3	Z_C	in	0.54
	Y_C	in	0.34
4	Z_C	in	0.41
	Y_C	in	0.63
5	Z_C	in	0.54
	Y_C	in	0.34

5.2 Equivalence Stiffness of Cross-section

The equivalent stiffness of the cross-section was derived in chapter 3. The result also compare with FEM.

5.2.1 Axial Stiffness

The axial stiffness can be calculated by the following equation.

$$\overline{\mathrm{EA}}_x = \frac{\mathrm{FL}}{2(\mathrm{U}_{x|at\ x=L/2})} \tag{5.3}$$

Where F is applied force along X-direction, L is total length of beam, U is deflection

The results were read at mid-length of the beam to avoid distortion from the boundary condition.

5.2.2 Bending Stiffness

For symmetrical geometry and symmetrical laminate, the bending moment about X-axis was applied and read the deflection. See the calculation method for bending stiffness at appendix A.

Table 5.3 Results of stiffnesses for all case

Case		Unit	Present	FEM	%Diff
ISO	$\overline{\overline{EA}}$	Lb	1.272E+06	1.276E+06	0.31
	$\overline{D}_x$	Lb-in^2	1.358E+05	1.358E+05	0.00
	$\overline{D}_y$	Lb-in^2	2.647E+05	2.646E+05	-0.04
	$\overline{D}_{xy}$	Lb-in^2	0	0	0
$[0]_{8T}$	$\overline{\overline{EA}}$	Lb	2.400E+06	2.400E+06	0
	$\overline{D}_x$	Lb-in^2	4.995E+05	4.990E+05	-0.10
	$\overline{D}_y$	Lb-in^2	2.563E+05	2.562E+05	-0.04
	$\overline{D}_{xy}$	Lb-in^2	0	0	0
$[\pm45°/0°/90°]_s$	$\overline{\overline{EA}}$	Lb	9.535E+05	9.562E+05	0.28
	$\overline{D}_x$	Lb-in^2	2.647E+05	2.646E+05	-0.04
	$\overline{D}_y$	Lb-in^2	1.359E+05	1.358E+05	-0.07
	$\overline{D}_{xy}$	Lb-in^2	0	0	0
$[\pm45°/0°/90°]_s$ Unsymmetrical geometry	$\overline{\overline{EA}}$	Lb	1.271E+06	1.275E+06	0.31
	$\overline{D}_x$	Lb-in^2	2.629E+05	2.650E+05	0.79
	$\overline{D}_y$	Lb-in^2	4.491E+05	4.485E+05	-0.13
	$\overline{D}_{xy}$	Lb-in^2	1.438E+05	1.448E+05	0.69
Unsymmetrical laminate	$\overline{\overline{EA}}$	Lb	9.382E+05	9.562E+05	1.88
	$\overline{D}_x$	Lb-in^2	1.972E+05	1.942E+05	-1.57
	$\overline{D}_y$	Lb-in^2	1.008E+05	1.027E+05	1.85
	$\overline{D}_{xy}$	Lb-in^2	0	0	0

5.3 Analysis of Ply Stresses

The stresses were obtained at the center point of each laminate throughout the thickness, point A, B and C are the mid-width of top flange, bottom flange and web, respectively (figure 5.1). For FEM, the cross section of the mid-length of beam was selected to avoid local influence in axial deflection due to loading and boundary condition on the both end of the beam.

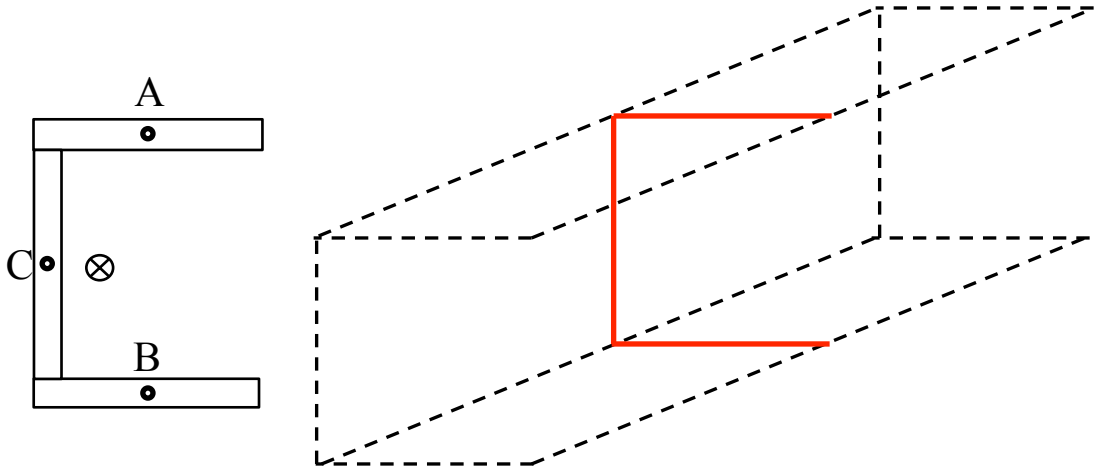

Figure 5.1 Points and cross-section for stress measurement

5.3.1 Isotropic Material

The first case is isotropic material with symmetric geometry. The isotropic material was study due to verify the model before going on composite material, unsymmetrical laminate and unsymmetrical geometry.

5.3.1.1 Axial Force with Isotropic material

Figure 5.2 illustrates the contour plot of structure deformation under axial force of 1 pound applied in X-direction acting the centroid.

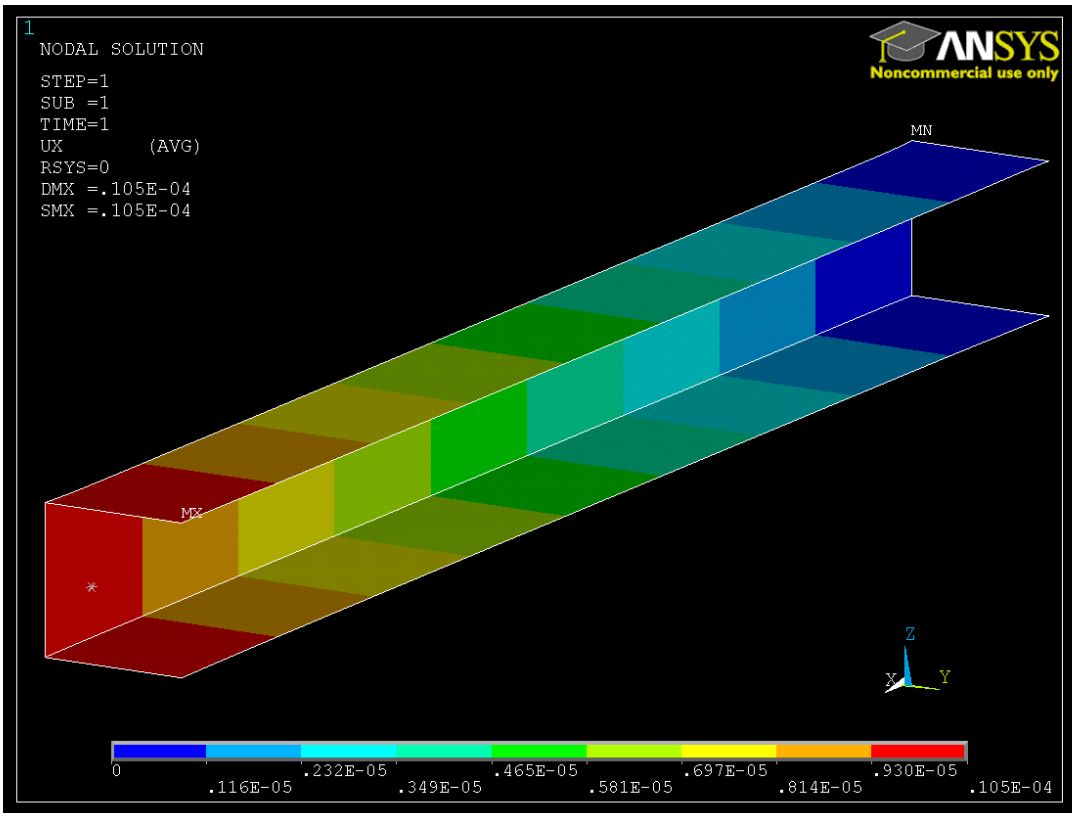

Figure 5.2 The displacement of C-channel beam under axial force at centroid

The ply stresses on the cross-section are the same because of the isotropic properties. The extension only occurred along the axial force. The stress results as expected must be the uniform along the cross-section. The stress results from present method (PM) exhibit excellent agreement with FEM results. Figure 5.3 show the the comparison of stress on both present method and finite element were plotted in graph form for each sub-laminate.

Table 5.4 Result of axial stresses under axial force for case 1 (Isotropic material)

Layer		Top Flange (psi)			Bottom Flange (psi)			Web (psi)		
		Present	FEM	% Diff	Present	FEM	% Diff	Present	FEM	% Diff
#8	Top	8.3333	8.3331	-0.0024	8.3333	8.3336	0.0036	8.3333	8.3332	-0.0012
	Bottom	8.3333	8.3332	-0.0012	8.3333	8.3335	0.0024	8.3333	8.3333	0
#7	Top	8.3333	8.3332	-0.0012	8.3333	8.3335	0.0024	8.3333	8.3333	0
	Bottom	8.3333	8.3332	-0.0012	8.3333	8.3334	0.0012	8.3333	8.3333	0
#6	Top	8.3333	8.3332	-0.0012	8.3333	8.3334	0.0012	8.3333	8.3333	0
	Bottom	8.3333	8.3333	0	8.3333	8.3334	0.0012	8.3333	8.3333	0
#5	Top	8.3333	8.3333	0	8.3333	8.3334	0.0012	8.3333	8.3333	0
	Bottom	8.3333	8.3333	0	8.3333	8.3333	0	8.3333	8.3333	0
#4	Top	8.3333	8.3333	0	8.3333	8.3333	0	8.3333	8.3333	0
	Bottom	8.3333	8.3334	0.0012	8.3333	8.3333	0	8.3333	8.3334	0.0012
#3	Top	8.3333	8.3334	0.0012	8.3333	8.3333	0	8.3333	8.3334	0.0012
	Bottom	8.3333	8.3334	0.0012	8.3333	8.3332	-0.0012	8.3333	8.3334	0.0012
#2	Top	8.3333	8.3334	0.0012	8.3333	8.3332	-0.0012	8.3333	8.3334	0.0012
	Bottom	8.3333	8.3335	0.0024	8.3333	8.3332	-0.0012	8.3333	8.3334	0.0012
#1	Top	8.3333	8.3335	0.0024	8.3333	8.3332	-0.0012	8.3333	8.3334	0.0012
	Bottom	8.3333	8.3336	0.0036	8.3333	8.3331	-0.0024	8.3333	8.3334	0.0012

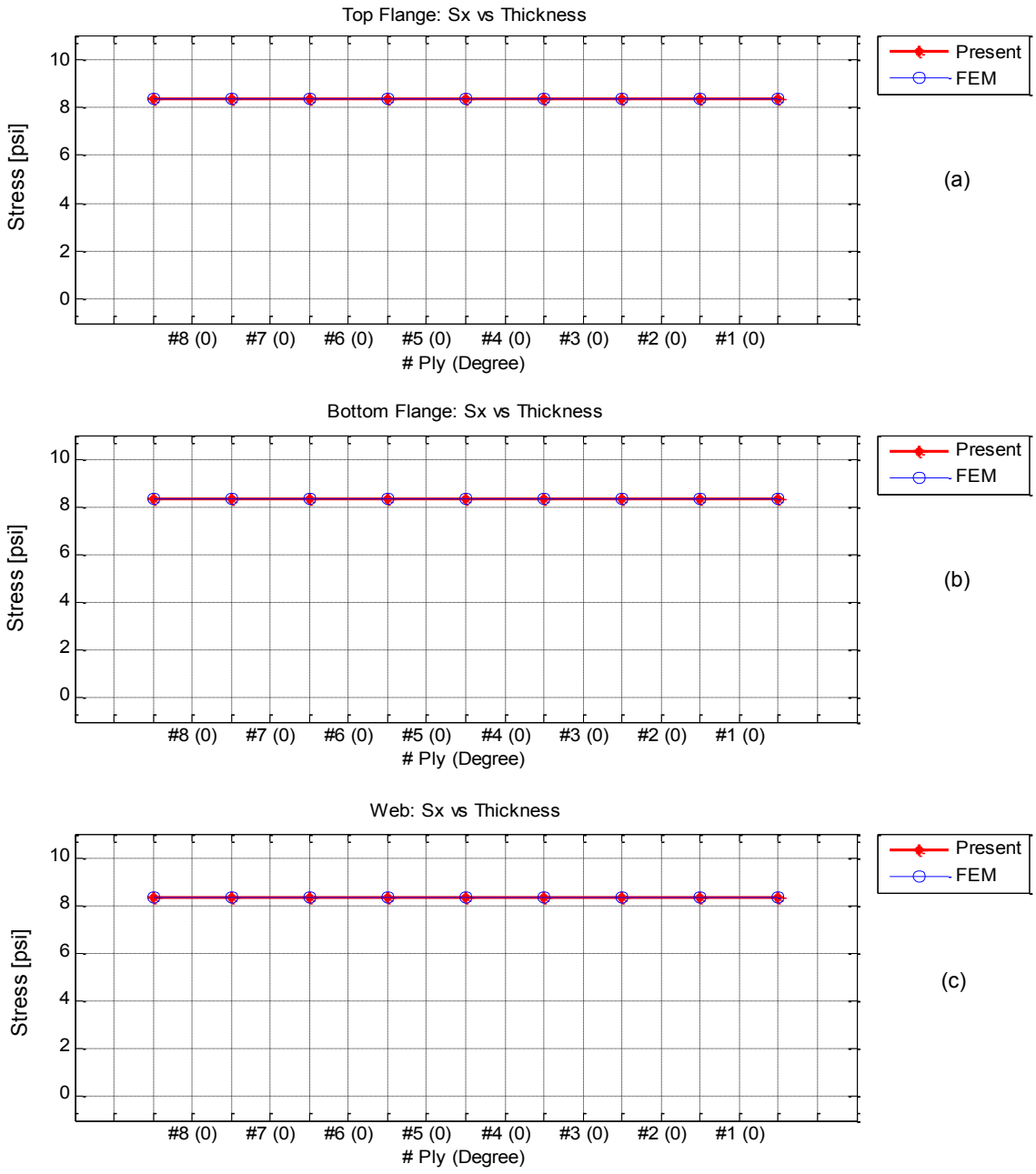

Figure 5.3 Axial stress on laminate for case 1 under axial force
(a) top flange (b) bottom flange (c) web

5.3.1.2 Bending Moment with Isotropic Material

The second study of the first case focused on bending moment about X-axis acting at the centroid. A 1 lb-in of bending moment was applied. Figure 5.1 illustrates the contour plot of structure deformation under bending moment.

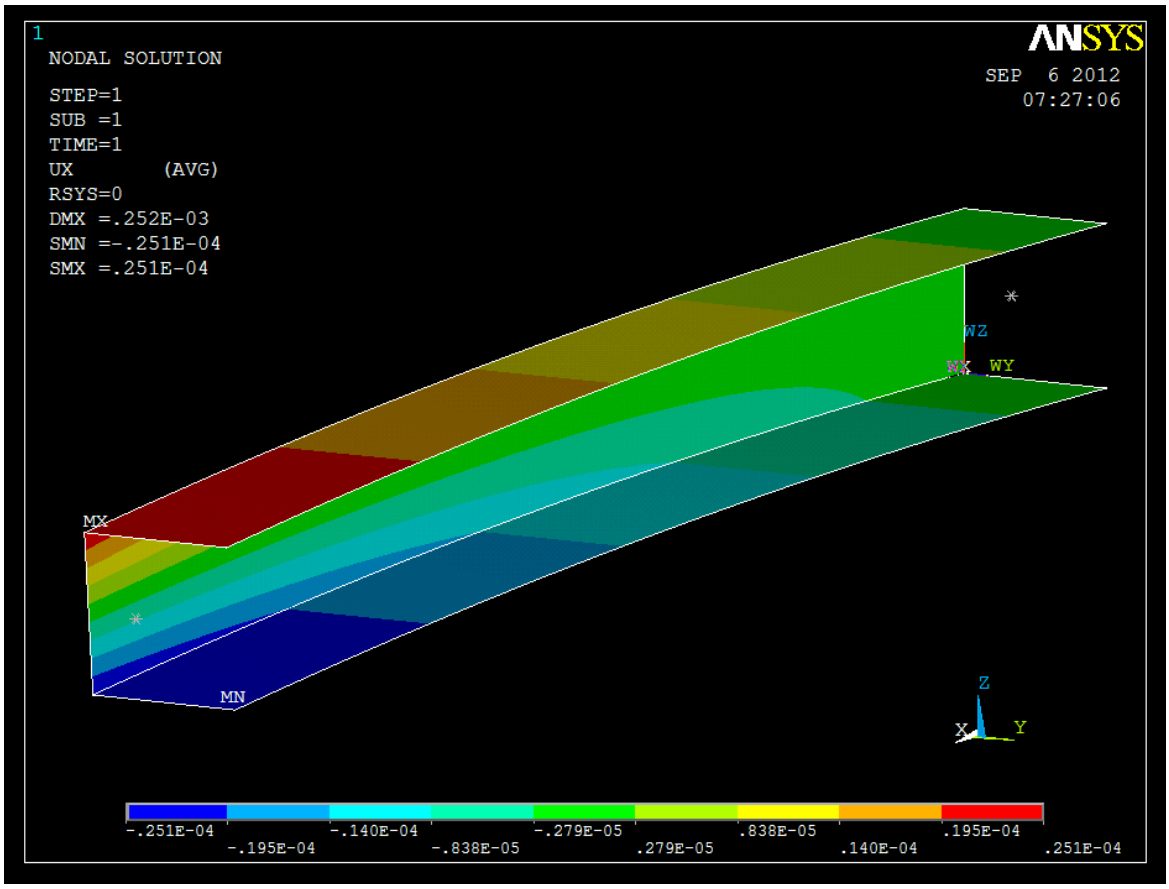

Figure 5.4 The displacement of C-channel beam under bending moment at centroid

The table 5.5 shows the axial stresses along the top and bottom flange are opposite direction. The most top of the top flange hold the maximum tension stress, while the most bottom of the bottom flange carried the maximum compression stress. There have no stress at the middle point of web which coincides with centroid about z-axis. The results also show that there has no coupling effect because the bending coupling stiffness is zero.

Since the results comparision between present method and FEM from axial force and bending moment case were perfectly match, the isotropic with C-channel model is validated. This model can use to other study by change the parametric, stacking sequence, and material property.

Table 5.5 Result of axial stresses under Bending Moment for case 1 (Isotropic material)

Layer		Top Flange (psi)			Bottom Flange (psi)		
		PM	FEM	%Diff	PM	FEM	%Diff
#8	T	21.621	21.621	0.000	-20.019	-20.020	0.005
	B	21.421	21.421	0.000	-20.219	-20.220	0.005
#7	T	21.421	21.421	0.000	-20.219	-20.220	0.005
	B	21.220	21.221	0.005	-20.420	-20.421	0.005
#6	T	21.220	21.221	0.005	-20.420	-20.421	0.005
	B	21.020	21.021	0.005	-20.620	-20.621	0.005
#5	T	21.020	21.021	0.005	-20.620	-20.621	0.005
	B	20.820	20.821	0.005	-20.820	-20.821	0.005
#4	T	20.820	20.821	0.005	-20.820	-20.821	0.005
	B	20.620	20.621	0.005	-21.020	-21.021	0.005
#3	T	20.620	20.621	0.005	-21.020	-21.021	0.005
	B	20.420	20.421	0.005	-21.220	-21.221	0.005
#2	T	20.420	20.421	0.005	-21.220	-21.221	0.005
	B	20.219	20.220	0.005	-21.421	-21.421	0.000
#1	T	20.219	20.220	0.005	-21.421	-21.421	0.000
	B	20.019	20.020	0.005	-21.621	-21.621	0.000

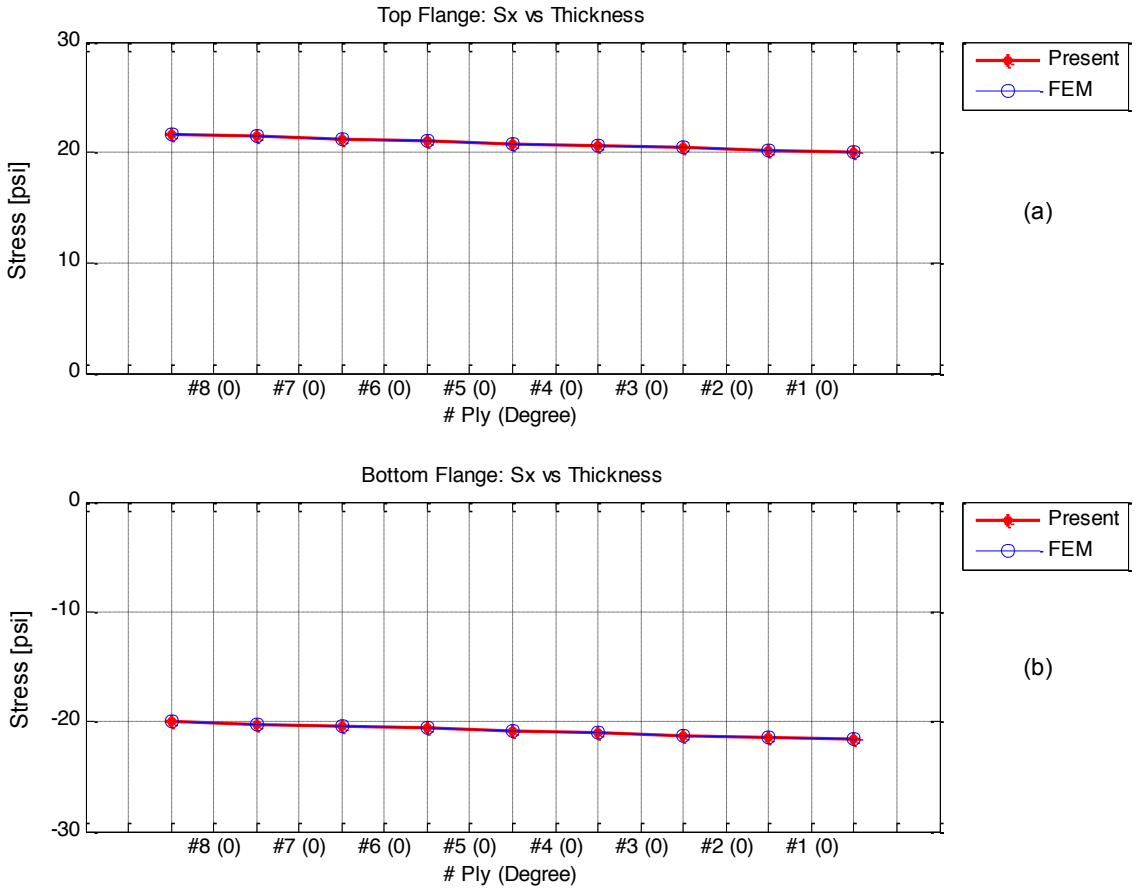

Figure 5.5 Axial stress on laminate for case 1 under bending moment
(a) top flange (b) bottom flange

5.3.2 Composite Material with all laminate layup are $[0^{\circ}]_{8T}$

From the first case, the material was changed from isotropic material to composite material (aluminum to AS/3501 graphite/epoxy). The all zero-degree plies were used to verify the model again. The study also expects the result as the isotropic material.

5.3.2.1 Axial Force with $[0°]_{8T}$

From table 5.6 the results expect the same as case 1. The composite material with all zero-degree plies exhibit like isotropic material. The stresses on the whole cross-section are uniform. The results from present method exhibit excellent agreement with FEM results. Figure 5.6 show the results of each sub-laminate under axial force.

Table 5.6 Result of axial stresses under axial force for case 2

Layer		Top Flange (psi)			Bottom Flange (psi)			Web (psi)		
		PM	FEM	%Diff	PM	FEM	%Diff	PM	FEM	%Diff
#8	T	8.3333	8.3325	-0.010	8.3333	8.3342	0.011	8.3333	8.3340	0.008
	B	8.3333	8.3327	-0.007	8.3333	8.3340	0.008	8.3333	8.3339	0.007
#7	T	8.3333	8.3327	-0.007	8.3333	8.3340	0.008	8.3333	8.3339	0.007
	B	8.3333	8.3329	-0.005	8.3333	8.3338	0.006	8.3333	8.3338	0.006
#6	T	8.3333	8.3329	-0.005	8.3333	8.3338	0.006	8.3333	8.3338	0.006
	B	8.3333	8.3332	-0.001	8.3333	8.3336	0.004	8.3333	8.3337	0.005
#5	T	8.3333	8.3332	-0.001	8.3333	8.3336	0.004	8.3333	8.3337	0.005
	B	8.3333	8.3334	0.001	8.3333	8.3334	0.001	8.3333	8.3336	0.004
#4	T	8.3333	8.3334	0.001	8.3333	8.3334	0.001	8.3333	8.3336	0.004
	B	8.3333	8.3336	0.004	8.3333	8.3332	-0.001	8.3333	8.3336	0.004
#3	T	8.3333	8.3336	0.004	8.3333	8.3332	-0.001	8.3333	8.3336	0.004
	B	8.3333	8.3338	0.006	8.3333	8.3329	-0.005	8.3333	8.3335	0.002
#2	T	8.3333	8.3338	0.006	8.3333	8.3329	-0.005	8.3333	8.3335	0.002
	B	8.3333	8.3340	0.008	8.3333	8.3327	-0.007	8.3333	8.3334	0.001
#1	T	8.3333	8.3340	0.008	8.3333	8.3327	-0.007	8.3333	8.3334	0.001
	B	8.3333	8.3342	0.011	8.3333	8.3325	-0.010	8.3333	8.3333	0.000

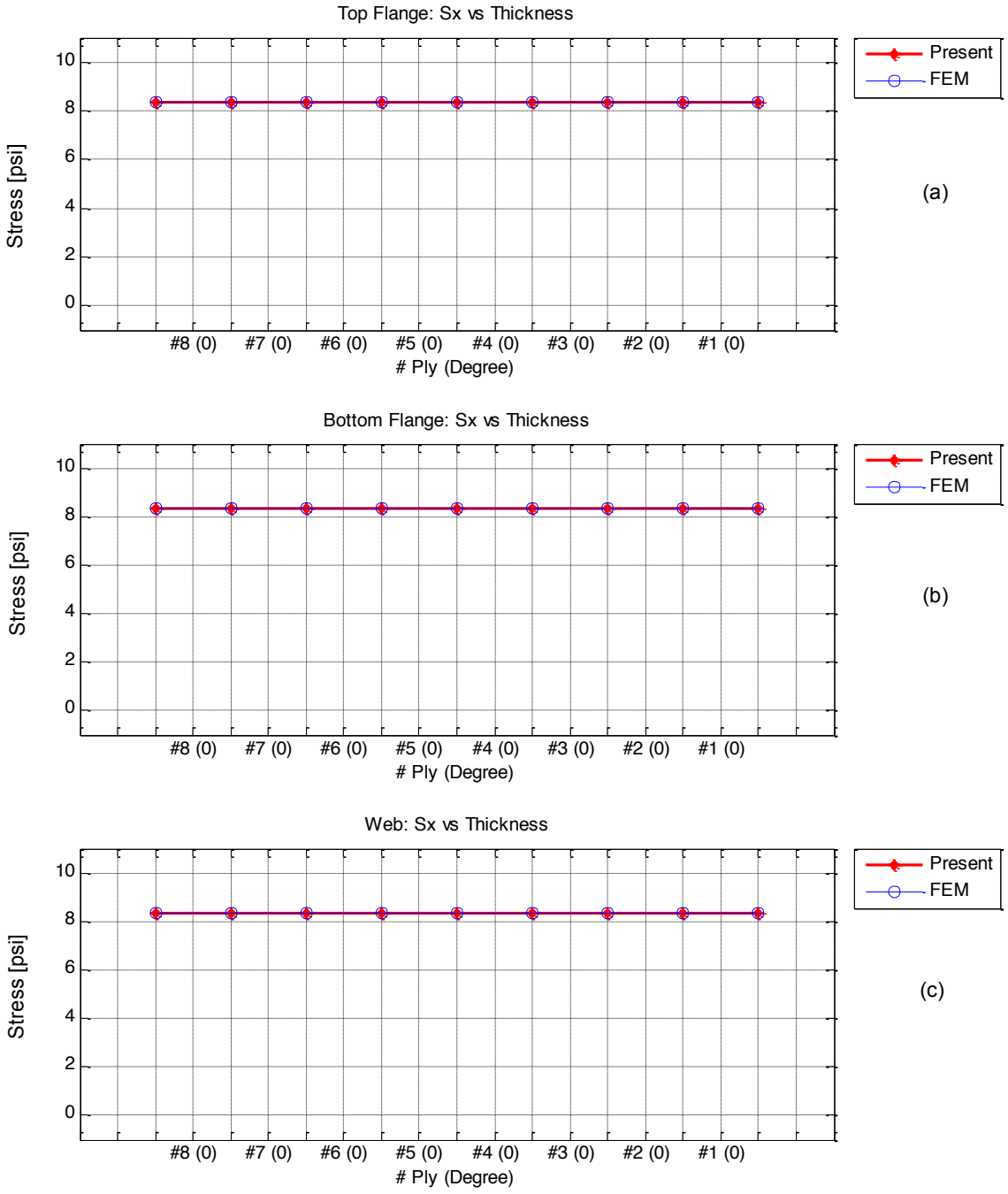

Figure 5.6 Axial stress on laminate for case 2 under axial force
(a) top flange (b) bottom flange (c) web

5.3.2.2 Bending Moment with $[0°]_{8T}$

The result from table 5.7 show that stresses from the all zero-degree plies are the same as the isotropic material. The axial stresses along the top and bottom flange are opposite direction and there have no stress on middle of the web. The results from present method exhibit excellent agreement with FEM results.

From isotropic material and composite material with $[0°]_{8T}$, the stresses results under axial force and bending moment of each case provided by present method exhibit excellent agreement with FEM results. The stresses distribution of all three sub-laminates lie straight thought out the thickness. The stresses were evaluated at the mid-width of each sub-laminated.

Table 5.7 Result of axial stresses under bending moment for case 2

Layer		Top Flange (psi)			Bottom Flange (psi)		
		PM	FEM	%Diff	PM	FEM	%Diff
#8	T	21.621	21.621	0.000	-20.019	-20.020	0.005
	B	21.421	21.421	0.000	-20.219	-20.220	0.005
#7	T	21.421	21.421	0.000	-20.219	-20.220	0.005
	B	21.220	21.221	0.005	-20.420	-20.421	0.005
#6	T	21.220	21.221	0.005	-20.420	-20.421	0.005
	B	21.020	21.021	0.005	-20.620	-20.621	0.005
#5	T	21.020	21.021	0.005	-20.620	-20.621	0.005
	B	20.820	20.821	0.005	-20.820	-20.821	0.005
#4	T	20.820	20.821	0.005	-20.820	-20.821	0.005
	B	20.620	20.621	0.005	-21.020	-21.021	0.005
#3	T	20.620	20.621	0.005	-21.020	-21.021	0.005
	B	20.420	20.421	0.005	-21.220	-21.221	0.005
#2	T	20.420	20.421	0.005	-21.220	-21.221	0.005
	B	20.219	20.220	0.005	-21.421	-21.421	0.000
#1	T	20.219	20.220	0.005	-21.421	-21.421	0.000
	B	20.019	20.020	0.005	-21.621	-21.621	0.000

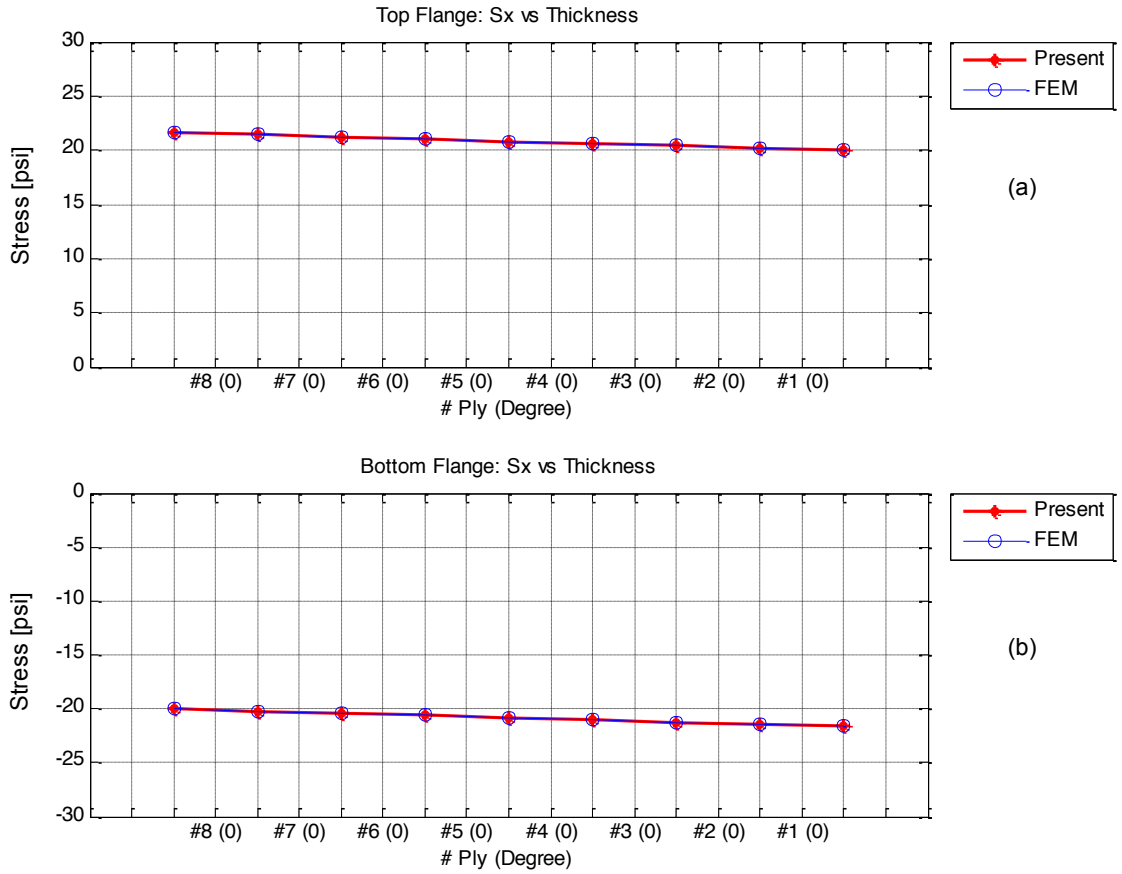

Figure 5.7 Axial stress on laminate for case 2 under bending moment
(a) top flange (b) bottom flange

5.3.3 Composite Material with all laminate layup are [±45°/0°/90°]s

5.3.3.1 Axial Force with [±45°/0°/90°]s

Table 5.8 lists the stresses, σ_x, of all the plies of the C-channel under an axial force. The results show all the stresses of a given ply either at the flanges or at the web have the same magnitude. It is also indicated that the 0°-ply carries the high stress while 90°-ply carries the least. These data are also plotted in Figure 5.8.

Table 5.8 Result of axial stresses under axial force for case 3

Layer		Top Flange (psi)			Bottom Flange (psi)			Web (psi)		
		PM	FEM	%Diff	PM	FEM	%Diff	PM	FEM	%Diff
#8 (45)	T	5.5459	5.553	0.122	5.5459	5.554	0.144	5.5459	5.553	0.121
	B	5.5459	5.553	0.124	5.5459	5.554	0.142	5.5459	5.553	0.122
#7 (-45)	T	5.5459	5.553	0.130	5.5459	5.553	0.135	5.5459	5.553	0.122
	B	5.5459	5.553	0.131	5.5459	5.553	0.135	5.5459	5.553	0.126
#6 (0)	T	20.961	20.973	0.057	20.961	20.973	0.057	20.961	20.973	0.057
	B	20.961	20.973	0.057	20.961	20.973	0.057	20.961	20.973	0.057
#5 (90)	T	1.281	1.254	-2.153	1.281	1.254	-2.153	1.281	1.254	-2.153
	B	1.281	1.254	-2.153	1.281	1.254	-2.153	1.281	1.254	-2.153
#4 (90)	T	1.281	1.254	-2.153	1.281	1.254	-2.153	1.281	1.254	-2.153
	B	1.281	1.254	-2.153	1.281	1.254	-2.153	1.281	1.254	-2.153
#3 (0)	T	20.961	20.973	0.057	20.961	20.973	0.057	20.961	20.973	0.057
	B	20.961	20.973	0.057	20.961	20.973	0.057	20.961	20.973	0.057
#2 (-45)	T	5.5459	5.553	0.135	5.5459	5.553	0.131	5.5459	5.554	0.139
	B	5.5459	5.553	0.135	5.5459	5.553	0.130	5.5459	5.554	0.142
#1 (45)	T	5.5459	5.554	0.140	5.5459	5.553	0.124	5.5459	5.554	0.142
	B	5.5459	5.554	0.142	5.5459	5.553	0.121	5.5459	5.554	0.146

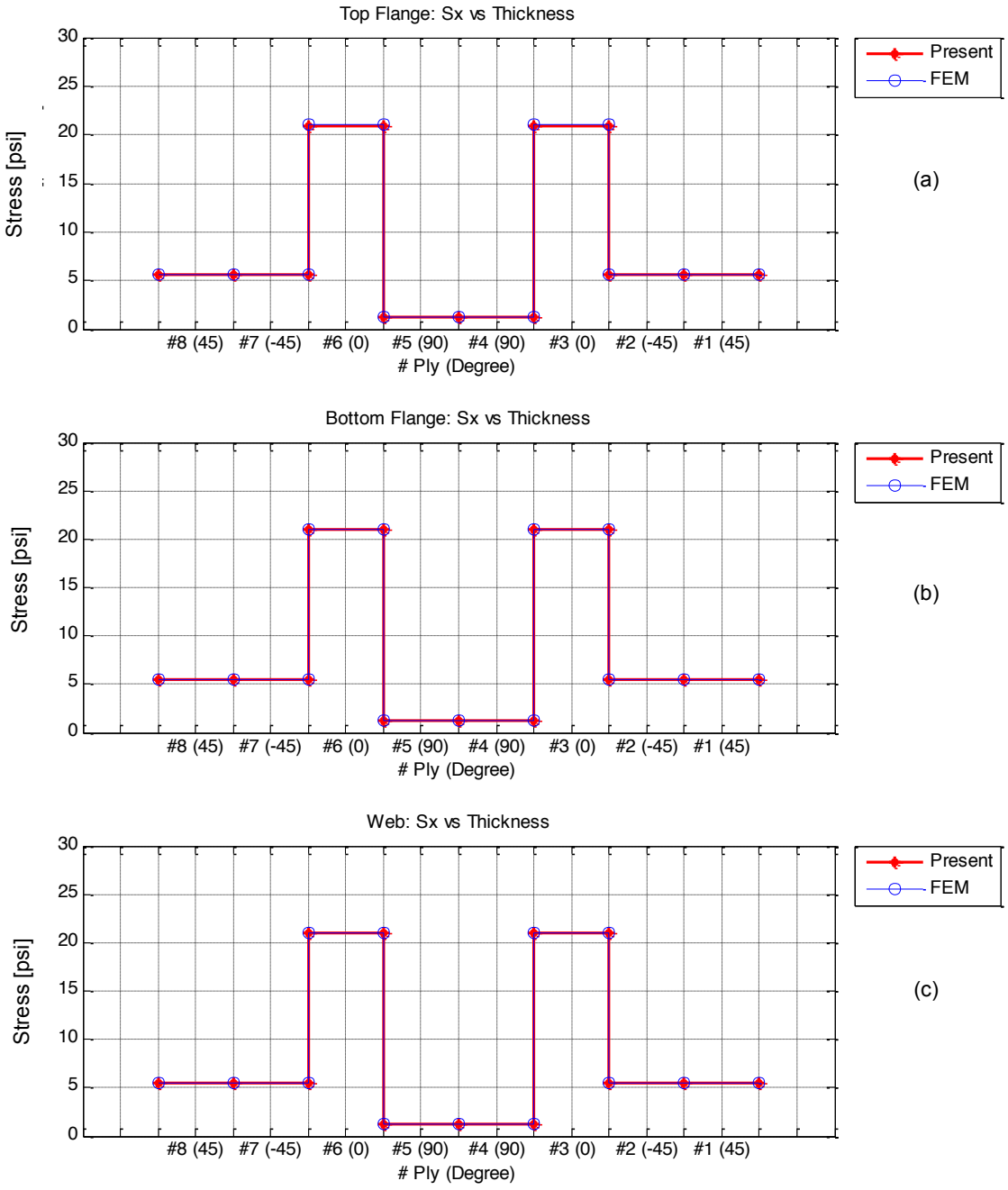

Figure 5.8 Axial stress on laminate for case 3 under axial force
(a) top flange (b) bottom flange (c) web

5.3.3.2 Bending Moment with [±45°/0°/90°]s

The results of stress in case 3 are shown on table 5.9. Stresses distributions on the top flange are tension stresses and bottom flange are compression stresses. Figure 5.8 clearly show the stresses distributions for the flange laminates by comparison between present method and FEM.

Table 5.9 Result of axial stresses under bending moment for case 3

Layer		Top Flange (psi)			Bottom Flange (psi)		
		PM	FEM	%Diff	PM	FEM	%Diff
8 (45)	T	14.2	14.2	0.1	-13.5	-13.5	0.1
	B	14.1	14.2	0.1	-13.6	-13.6	0.1
7 (-45)	T	14.1	14.2	0.2	-13.6	-13.6	0.1
	B	14.0	14.1	0.2	-13.7	-13.7	0.1
6 (0)	T	53.4	53.4	0.1	-51.4	-51.4	0.1
	B	52.9	52.9	0.1	-51.9	-51.9	0.1
5 (90)	T	3.2	3.2	-2.2	-3.2	-3.1	-2.0
	B	3.2	3.1	-2.1	-3.2	-3.1	-2.1
4 (90)	T	3.2	3.1	-2.1	-3.2	-3.1	-2.1
	B	3.2	3.1	-2.0	-3.2	-3.2	-2.2
3 (0)	T	51.9	51.9	0.1	-52.9	-52.9	0.1
	B	51.4	51.4	0.1	-53.4	-53.4	0.1
2 (-45)	T	13.7	13.7	0.1	-14.0	-14.1	0.2
	B	13.6	13.6	0.1	-14.1	-14.2	0.2
1 (45)	T	13.6	13.6	0.1	-14.1	-14.2	0.1
	B	13.5	13.5	0.1	-14.2	-14.2	0.1

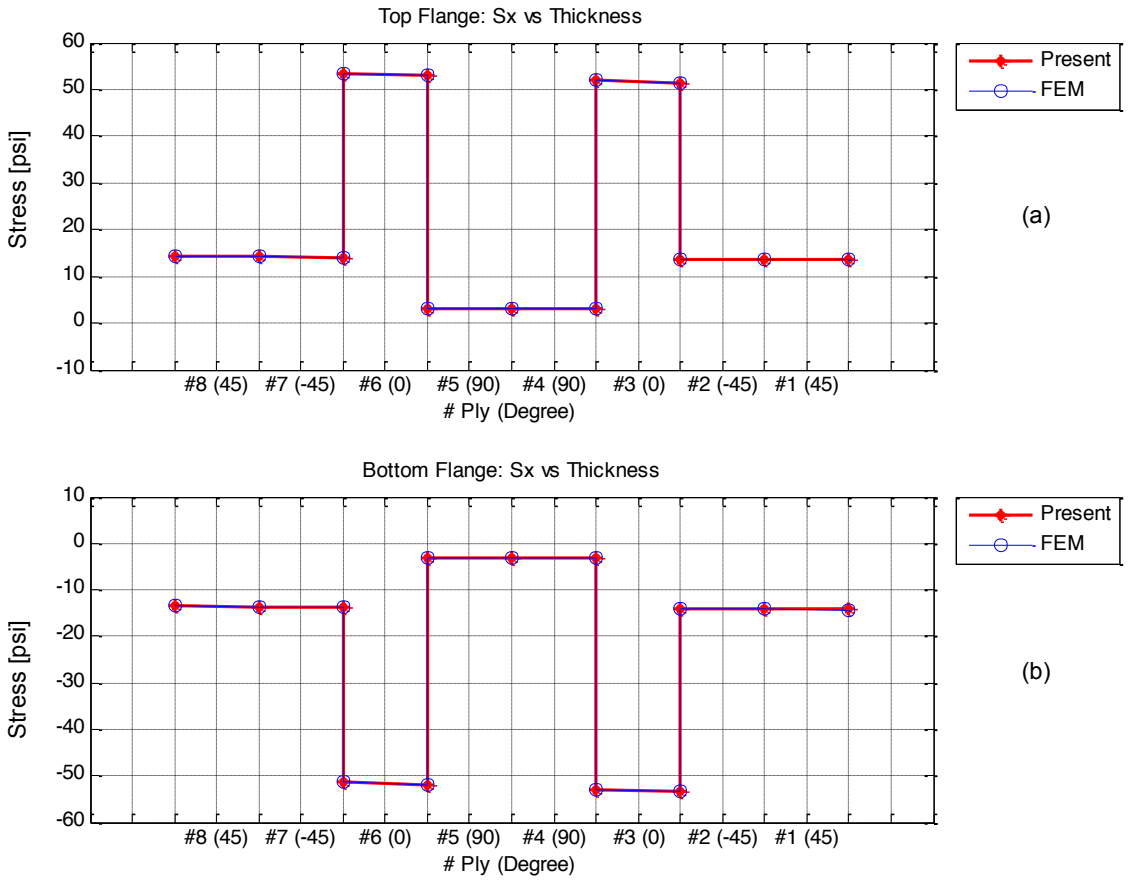

Figure 5.9 Axial stress on laminate for case 3 under bending moment
(a) top flange (b) bottom flange

For cross-section stress distribution, the outer zero-degree ply of the flange laminates (see Figure 5.11) was selected to read the stresses. The cross-section was divided into 31 points, each sub laminated were divided into 11 points along their width.

- Top flange : from free end to top corner (1 to 11)
- Web : from top corner to bottom corner (11 to 21)
- Bottom flange : from bottom corner to free end (21 to 31)

The point 11 is the connection point of top flange and web, and 21 is the connection point of web and bottom flange. The Figure 5.10 showed the point locations which were selected to read the result. The red area represents the outer zero-degree ply.

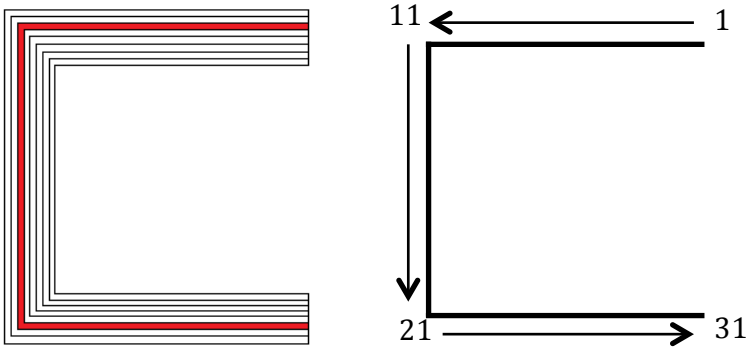

Figure 5.10 Location of selected point along C-channel cross-section

Form table 5.10 show the stresses distribution along C-channel cross-section. The stresses along top flange are tension stresses while the bottom flange are compression stresses. Consider stresses along the web, the half top above centroid line are tension stress as top flange, while the half bottom under centroid line are compression stress as bottom flange. The results from both present method (PM) and FEM are perfectly agreed. Figure 5.11 is the results show the perfectly image of stresses distribution along the cross-section.

Table 5.10 Axial stresses along zero-degree ply under bending moment for case 3

Top Flange (psi)				Bottom Flange (psi)				Web (psi)			
point	PM	FEM	%Diff	point	PM	FEM	%Diff	point	PM	FEM	%Diff
1	52.88	52.93	0.1	11	52.88	51.63	-2.41	21	-52.88	-51.63	-2.41
2	52.88	52.93	0.09	12	40.29	40.3	0.03	22	-52.88	-52.89	0.03
3	52.88	52.92	0.09	13	30.22	30.23	0.03	23	-52.88	-52.9	0.04
4	52.88	52.92	0.08	14	20.14	20.15	0.03	24	-52.88	-52.9	0.05
5	52.88	52.91	0.07	15	10.07	10.08	0.03	25	-52.88	-52.91	0.05
6	52.88	52.91	0.06	16	0	0	0	26	-52.88	-52.91	0.06
7	52.88	52.91	0.05	17	-10.07	-10.08	0.03	27	-52.88	-52.91	0.07
8	52.88	52.9	0.05	18	-20.15	-20.15	0	28	-52.88	-52.92	0.08
9	52.88	52.9	0.04	19	-30.23	-30.23	0	29	-52.88	-52.92	0.09
10	52.88	52.89	0.03	20	-40.3	-40.3	0	30	-52.88	-52.93	0.09
11	52.88	51.63	-2.41	21	-52.88	-51.63	-2.41	31	-52.88	-52.93	0.1

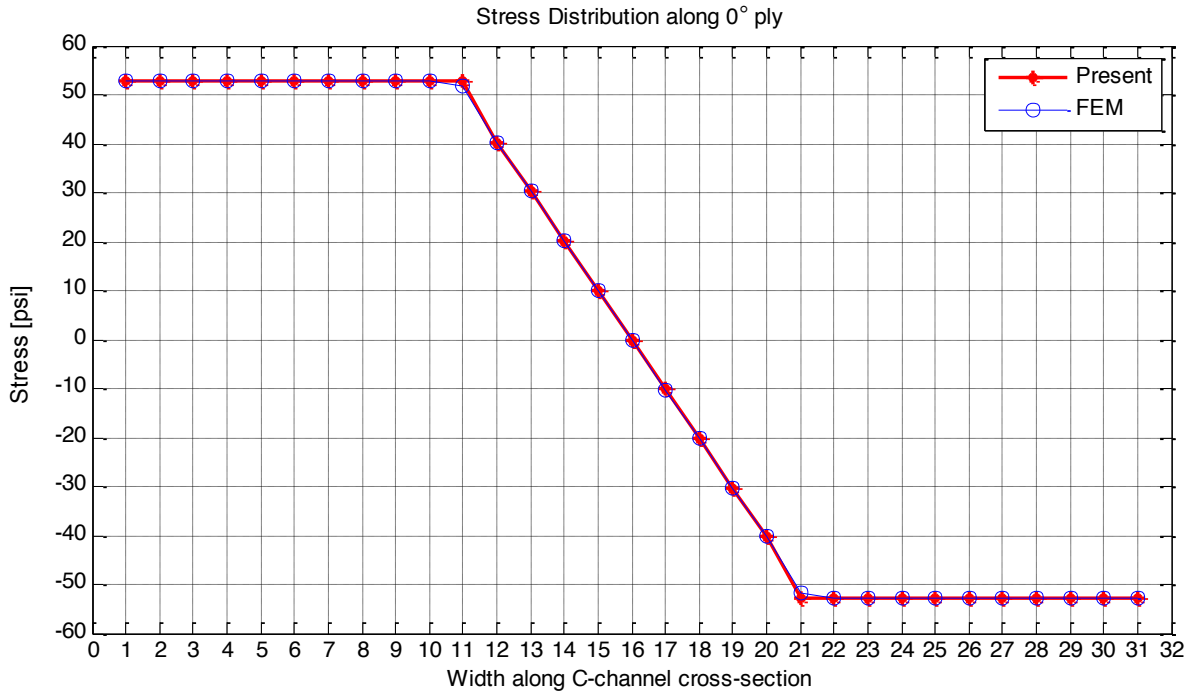

Figure 5.11 Stress distributions along zero-degree ply of cross-section case 3

5.3.4 Composite Material with Unsymmetrical Geometry

For unsymmetrical geometry case, the width of the bottom flange was changed from one inch to two inches.

5.3.4.1 Axial Force with Unsymmetrical Geometry

The result from Table 5.11 shows the stresses for unsymmetrical geometric case. The stresses are uniform distributed on the same angle ply. The stresses are uniform over their own angle ply. Figure 5.12 clearly shows the stresses distributions for all sub-laminates obtained by both present method and FEM. A 1 pound of axial force was applied at the centroid of cross-section.

Table 5.11 Result of axial stresses under axial force for case 4

Layer		Top Flange (psi)			Bottom Flange (psi)			Web (psi)		
		PM	FEM	%Diff	PM	FEM	%Diff	PM	FEM	%Diff
8 (45)	T	4.16	4.16	-0.05	4.16	4.17	0.27	4.16	4.16	0.11
	B	4.16	4.16	-0.05	4.16	4.17	0.26	4.16	4.16	0.12
7 (-45)	T	4.16	4.16	-0.04	4.16	4.17	0.26	4.16	4.16	0.12
	B	4.16	4.16	-0.04	4.16	4.17	0.25	4.16	4.17	0.13
6 (0)	T	15.72	15.70	-0.12	15.72	15.74	0.15	15.72	15.73	0.08
	B	15.72	15.70	-0.12	15.72	15.74	0.14	15.72	15.73	0.08
5 (90)	T	0.96	0.94	-2.34	0.96	0.94	-2.07	0.96	0.94	-2.14
	B	0.96	0.94	-2.34	0.96	0.94	-2.08	0.96	0.94	-2.14
4 (90)	T	0.96	0.93	-2.88	0.96	0.94	-2.09	0.96	0.94	-2.14
	B	0.96	0.94	-2.34	0.96	0.94	-2.09	0.96	0.94	-2.14
3 (0)	T	15.72	15.70	-0.12	15.72	15.74	0.13	15.72	15.73	0.08
	B	15.72	15.70	-0.12	15.72	15.74	0.13	15.72	15.73	0.08
2 (-45)	T	4.16	4.16	-0.04	4.16	4.17	0.18	4.16	4.17	0.17
	B	4.16	4.16	-0.05	4.16	4.17	0.16	4.16	4.17	0.18
1 (45)	T	4.16	4.16	-0.04	4.16	4.17	0.17	4.16	4.17	0.18
	B	4.16	4.16	-0.04	4.16	4.17	0.15	4.16	4.17	0.19

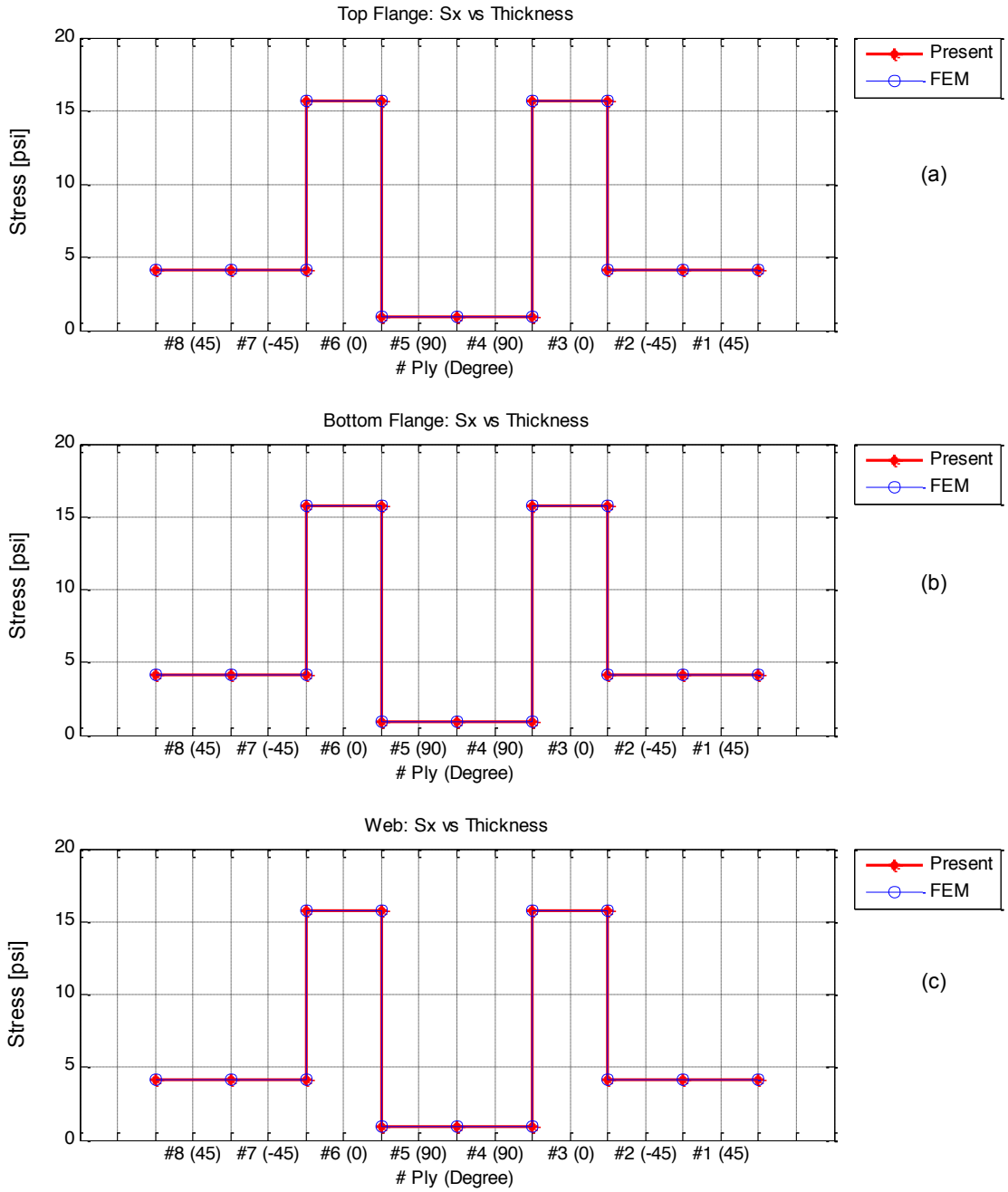

Figure 5.12 Axial stress on laminate for case 4 under axial force
(a) top flange (b) bottom flange (c) web

5.3.4.2 Bending Moment with Unsymmetrical Geometry

A 1 lb-in of bending moment was applied at the centroid of cross-section. Table 5.12 lists the stress results for unsymmetrical geometry. Figure 5.13 clearly show the stresses distributions for the flange laminates by comparison between present method and FEM.

Table 5.12 Result of axial stresses under bending moment for case 4

Layer		Top Flange (psi)			Bottom Flange (psi)		
		PM	FEM	%Diff	PM	FEM	%Diff
8 (45)	T	15.17	15.19	0.09	-6.28	-6.24	-0.69
	B	15.09	15.10	0.10	-6.37	-6.34	-0.49
7 (-45)	T	15.09	15.11	0.17	-6.37	-6.34	-0.42
	B	15.00	15.03	0.17	-6.45	-6.44	-0.22
6 (0)	T	56.98	57.02	0.06	-24.11	-24.10	-0.02
	B	56.52	56.56	0.06	-24.46	-24.57	0.46
5 (90)	T	3.45	3.38	-2.17	-1.50	-1.47	-3.95
	B	3.43	3.35	-2.15	-1.53	-1.50	-2.16
4 (90)	T	3.43	3.35	-2.15	-1.53	-1.50	-2.16
	B	3.40	3.33	-2.12	-1.56	-1.52	-2.12
3 (0)	T	55.61	55.64	0.07	-25.48	-25.50	0.09
	B	55.15	55.19	0.07	-25.94	-25.73	-0.80
2 (-45)	T	14.67	14.69	0.15	-6.79	-6.82	0.50
	B	14.58	14.60	0.15	-6.87	-6.92	0.67
1 (45)	T	14.58	14.60	0.14	-6.87	-6.92	0.64
	B	14.50	14.52	0.15	-6.96	-7.02	0.81

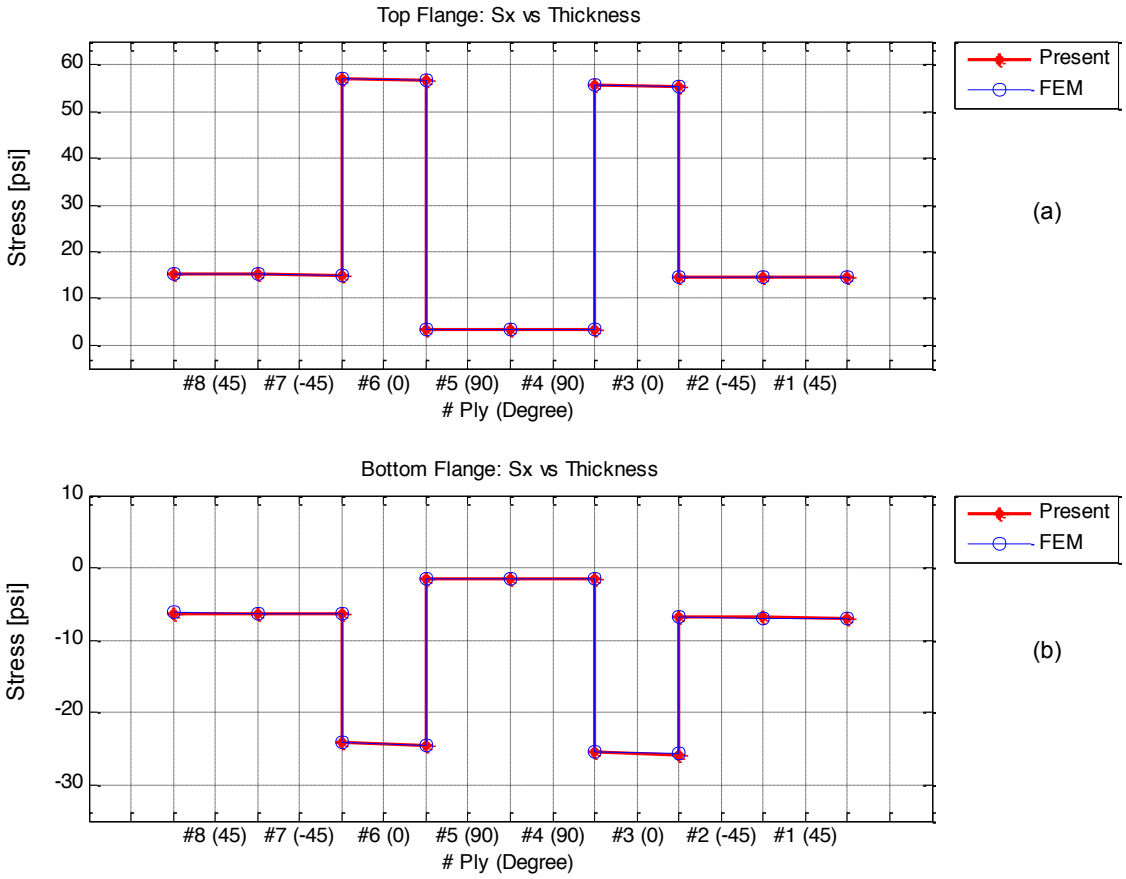

Figure 5.13 Axial stress on laminate for case 4 under bending moment
(a) top flange (b) bottom flange

For cross-section stress distribution, the outer zero-degree ply was also select to read the stresses. Table 5.13 lists the results of stress on outer zero-degree ply. Figure 5.14 shows the results that is an excellent agreement with the results obtained from FEM.

Table 5.13 Axial stresses along zero-degree ply under bending moment for case 4

Top Flange (psi)				Bottom Flange (psi)				Web (psi)			
point	PM	FEM	%Diff	point	PM	FEM	%Diff	point	PM	FEM	%Diff
1	71.28	71.35	0.10	11	41.77	40.84	-2.27	21	-54.99	-53.49	-2.80
2	68.33	68.39	0.09	12	30.70	30.70	0.00	22	-49.09	-49.11	0.04
3	65.38	65.43	0.09	13	21.48	21.48	-0.01	23	-43.19	-43.21	0.05
4	62.42	62.47	0.08	14	12.26	12.26	-0.03	24	-37.28	-37.30	0.05
5	59.47	59.52	0.07	15	3.05	3.04	-0.21	25	-31.38	-31.40	0.07
6	56.52	56.56	0.06	16	-6.17	-6.17	0.14	26	-25.48	-25.50	0.09
7	53.57	53.60	0.05	17	-15.38	-15.39	0.07	27	-19.58	-19.60	0.13
8	50.62	50.64	0.04	18	-24.60	-24.61	0.05	28	-13.68	-13.71	0.20
9	47.67	47.69	0.03	19	-33.81	-33.83	0.05	29	-7.78	-7.81	0.38
10	44.72	44.73	0.02	20	-43.03	-43.05	0.04	30	-1.87	-1.91	1.73
11	41.77	40.84	-2.27	21	-54.99	-53.49	-2.80	31	4.03	3.99	-0.89

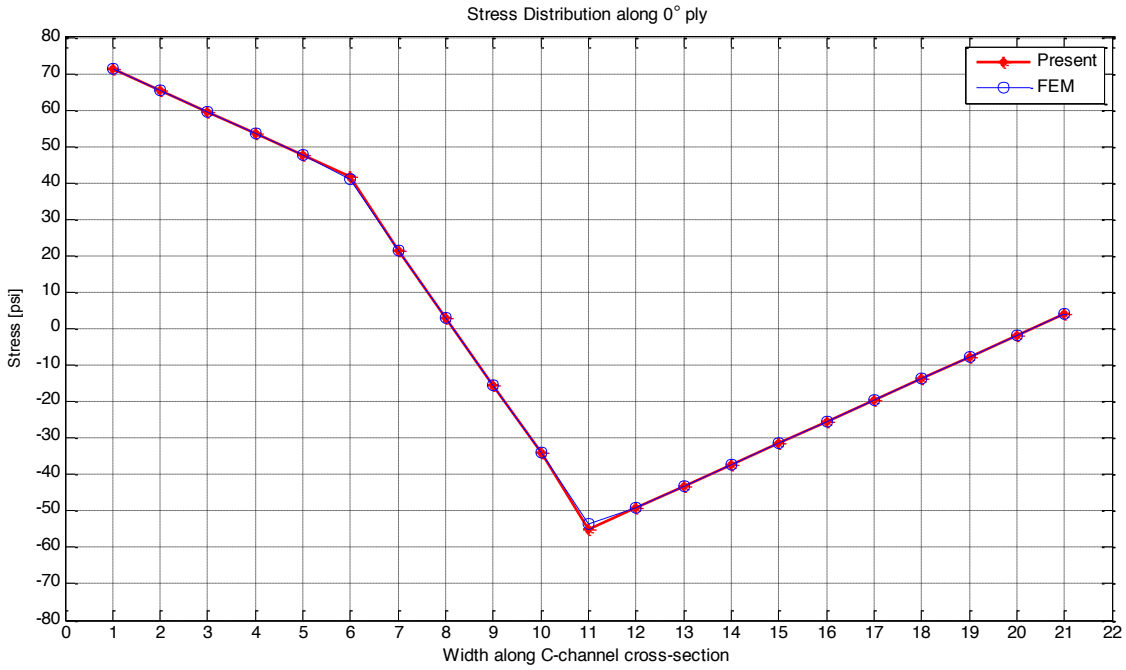

Figure 5.14 Stress distributions along zero-degree ply of cross-section case 4

5.3.5 Composite Material with Unsymmetrical Laminate

For the unsymmetrical laminate case, the beam consists of a top flange and web of [0/45/-45/90/45/0/-45/90] and bottom flange of [90/-45/0/45/90/-45/45/0]. The coupling stiffness will affect the stresses over the cross-section.

5.3.5.1 Axial Force with Unsymmetrical Laminate

Table 5.14 shows the results for axial stress for all plies, the zero-degree ply also deal with the maximum induced stress. Consider only four stresses result on zero-degree ply, there are no longer uniform due to the coupling effect on each sub-laminate. Because of the unsymmetrical laminate, the centroid of each sub-laminates don't locate on the centerline, so their will induce coupling effect on each sub-laminate. Figure 5.15 shows the stress distribution of each sub-laminate.

Table 5.14 Result of axial stresses under axial force for case 5

Layer		Top Flange (psi)			Bottom Flange (psi)			Web (psi)		
		PM	FEM	%Diff	PM	FEM	%Diff	PM	FEM	%Diff
#8	T	21.22	21.64	1.94	1.36	1.33	-2.70	21.22	21.25	0.13
	B	21.24	21.65	1.89	1.34	1.30	-3.10	21.24	21.27	0.18
#7	T	4.80	4.82	0.49	6.08	6.00	-1.29	4.80	4.78	-0.45
	B	5.07	5.11	0.86	5.81	5.72	-1.58	5.07	5.06	-0.06
#6	T	4.75	4.90	2.97	21.33	20.95	-1.89	4.75	4.79	0.83
	B	5.02	5.15	2.60	21.31	20.93	-1.80	5.02	5.04	0.55
#5	T	1.27	1.26	-1.13	5.86	5.77	-1.64	1.27	1.24	-2.69
	B	1.29	1.28	-0.73	5.60	5.52	-1.38	1.29	1.26	-2.20
#4	T	5.60	5.68	1.48	1.29	1.23	-4.41	5.60	5.63	0.61
	B	5.86	5.97	1.75	1.27	1.21	-4.88	5.86	5.92	0.90
#3	T	21.31	21.68	1.72	5.02	4.89	-2.66	21.31	21.38	0.36
	B	21.33	21.69	1.68	4.75	4.61	-3.11	21.33	21.41	0.40
#2	T	5.81	5.91	1.68	5.07	5.03	-0.78	5.81	5.81	-0.15
	B	6.08	6.17	1.43	4.80	4.78	-0.44	6.08	6.06	-0.34
#1	T	1.34	1.35	0.43	21.24	20.87	-1.75	1.34	1.33	-0.81
	B	1.36	1.37	0.79	21.22	20.86	-1.75	1.36	1.36	-0.38

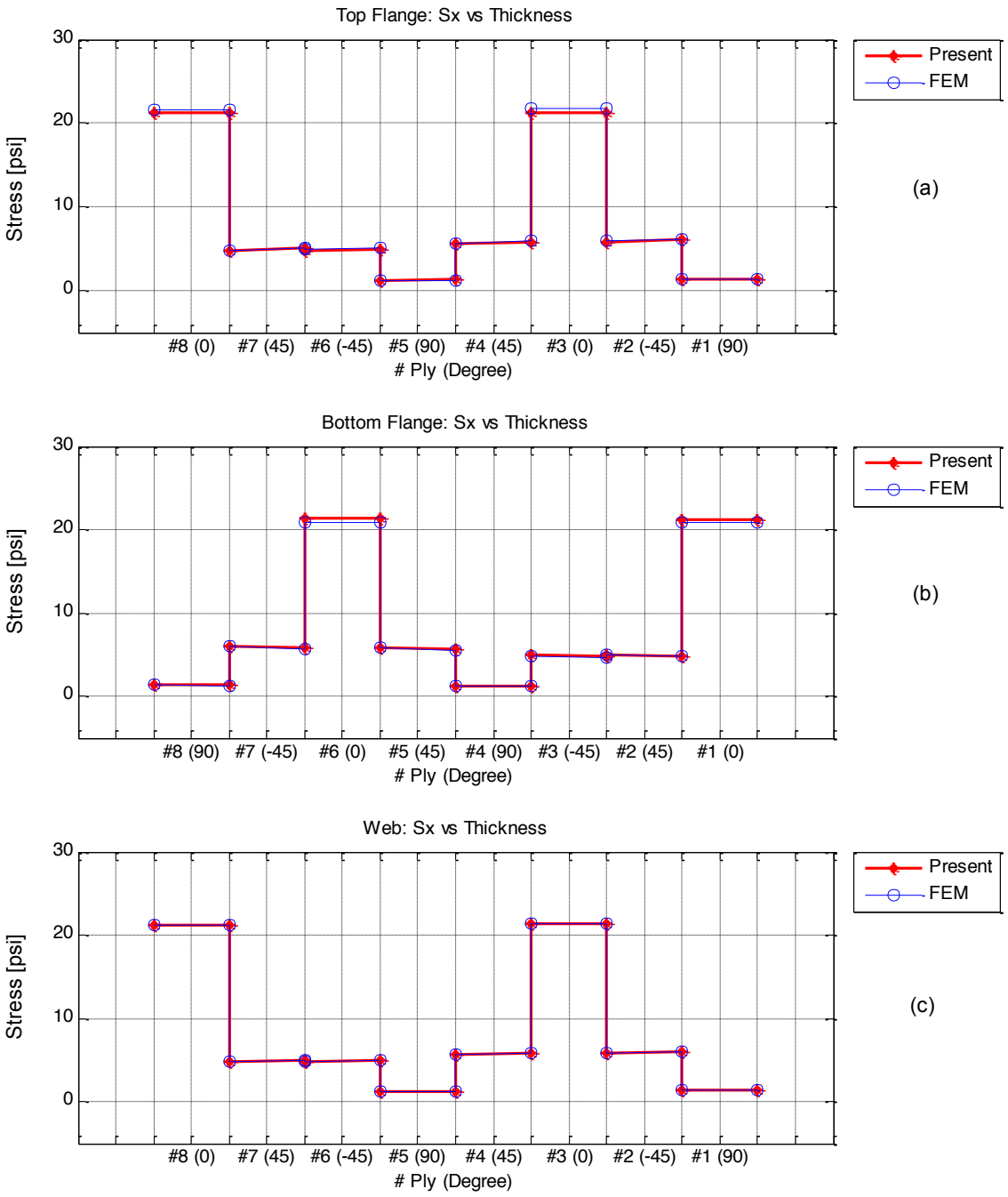

Figure 5.15 Axial stress on laminate for case 5 under axial force
(a) top flange (b) bottom flange (c) web

5.3.5.2 Bending Moment with Unsymmetrical Laminate

The stress results were shown on table 5.15 and figure 5.16.

Table 5.15 Result of axial stresses under bending moment for case 5

Layer		Top Flange (psi)			Layer		Bottom Flange (psi)		
		PM	FEM	%Diff			PM	FEM	%Diff
#8 (0°)	T	54.51	54.60	0.17	#8 (90°)	T	-3.24	-3.22	-0.44
	B	54.05	54.15	0.19		B	-3.22	-3.20	-0.90
#7 (45°)	T	12.22	11.90	-2.65	#7 (-45°)	T	-14.64	-14.61	-0.23
	B	12.73	12.51	-1.80		B	-14.12	-14.15	0.18
#6 (-45°)	T	12.06	12.32	2.12	#6 (0°)	T	-51.73	-51.86	0.25
	B	12.57	12.78	1.59		B	-52.20	-52.32	0.23
#5 (90°)	T	3.17	3.09	-2.79	#5 (45°)	T	-14.28	-14.32	0.27
	B	3.19	3.11	-2.29		B	-13.77	-13.72	-0.37
#4 (45°)	T	13.77	13.72	-0.34	#4 (90°)	T	-3.19	-3.11	-2.33
	B	14.28	14.33	0.29		B	-3.17	-3.09	-2.82
#3 (0°)	T	52.20	52.33	0.26	#3 (-45°)	T	-12.57	-12.77	1.56
	B	51.73	51.88	0.28		B	-12.06	-12.31	2.09
#2 (-45°)	T	14.12	14.15	0.21	#2 (45°)	T	-12.73	-12.50	-1.83
	B	14.64	14.61	-0.20		B	-12.22	-11.90	-2.67
#1 (90°)	T	3.22	3.20	-0.87	#1 (0°)	T	-54.05	-54.13	0.15
	B	3.24	3.22	-0.41		B	-54.51	-54.58	0.14

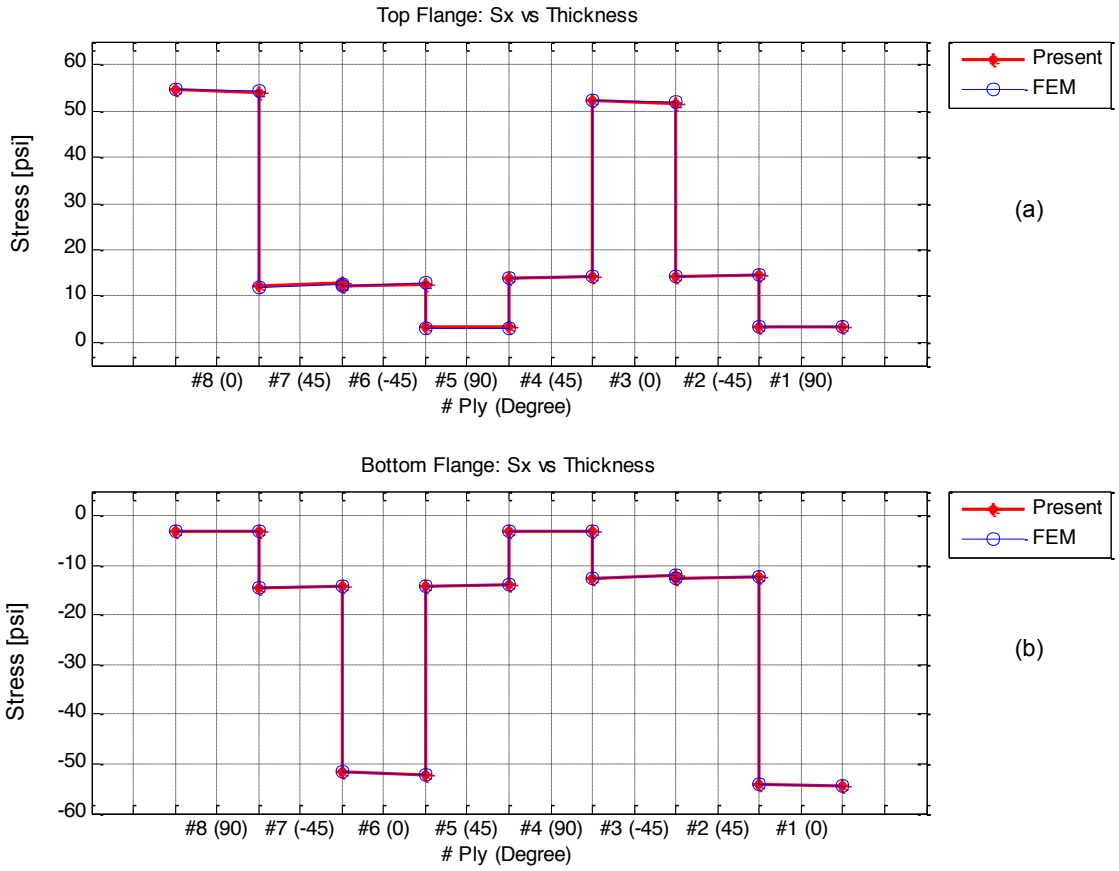

Figure 5.16 Axial stress on laminate for case 5 under bending moment
(a) top flange (b) bottom flange

For cross-section stress distribution, the bottom of inner zero-degree ply was select to read the stresses. The cross-section was divided into 31 points, each sub laminated were divided into 11 points along their width. Table 5.16 lists the results of stress on outer zero-degree ply. Figure 5.17 is the results show the perfectly image of stresses distribution along the cross-section.

Table 5.16 Axial stresses along zero-degree ply under bending moment for case 5

Top Flange (psi)				Bottom Flange (psi)				Web (psi)			
point	PM	FEM	%Diff	point	PM	FEM	%Diff	point	PM	FEM	%Diff
1	51.73	52.07	0.65	11	51.73	51.49	-0.48	21	-51.73	-51.75	0.04
2	51.73	52.08	0.67	12	40.58	40.69	0.28	22	-51.73	-52.07	0.64
3	51.73	52.09	0.68	13	30.43	30.52	0.30	23	-51.73	-52.07	0.66
4	51.73	52.09	0.69	14	20.29	20.36	0.35	24	-51.73	-52.08	0.67
5	51.73	52.10	0.70	15	10.14	10.20	0.51	25	-51.73	-52.09	0.68
6	51.73	52.11	0.71	16	0.00	0.03	100	26	-51.73	-52.09	0.68
7	51.73	52.11	0.72	17	-10.14	-10.13	-0.11	27	-51.73	-52.09	0.69
8	51.73	52.11	0.73	18	-20.29	-20.30	0.04	28	-51.73	-52.10	0.70
9	51.73	52.12	0.74	19	-30.43	-30.45	0.05	29	-51.73	-52.10	0.70
10	51.73	52.12	0.74	20	-40.58	-40.63	0.12	30	-51.73	-52.10	0.70
11	51.73	51.49	-0.48	21	-51.73	-51.75	0.04	31	-51.73	-52.10	0.71

Figure 5.17 Stress distributions along zero-degree ply of cross-section case 5

CHAPTER 6

CONCLUSION AND FUTURE WORK

An analytical closed-form solution for analyzing laminated composite beam with C-channel cross-section is developed to obtain the centroid, axial and bending stiffness and ply stresses. The present method was developed base on extension of classical lamination theory and the characteristic behavior of narrow beam. C-channel with symmetric and unsymmetrical layups and equal and unequal width of the top/bottom flanges are investigated. An ANSYS model is also developed to obtain all of the results which are used for comparison.

For all the cases studied, the ply stresses and axial and bending stiffness obtained from the present method show excellent agreement with the results obtained from ANSYS. The stress results also indicate that the uniform stress distribution of 0°-ply of the top and bottom flange is obtained for equal width of C-channel regardless the symmetric and unsymmetrical layup. For unequal width of the flanges of C-channel, the stresses distribution of 0°-ply is quite different between the top and bottom flange. This is because the bending moment is applied at the centroid. The torque is induced that causes the rotation of C-channel.

In future studies, the analysis could be extended to include the behavior under torsion, determination of shear center, and the interlamina shear for C-channel cross-section subjected to a transverse load.

It should be noted that the present method can be easily applied to conduct the parametric study in stress analysis of C-channel.

APPENDIX A

CALCULATION OF CURVATURE of CURVED BEAM FROM FINITE ELEMENT METHOD

The procedure to obtain the curvature of the curved beam by finite element method.

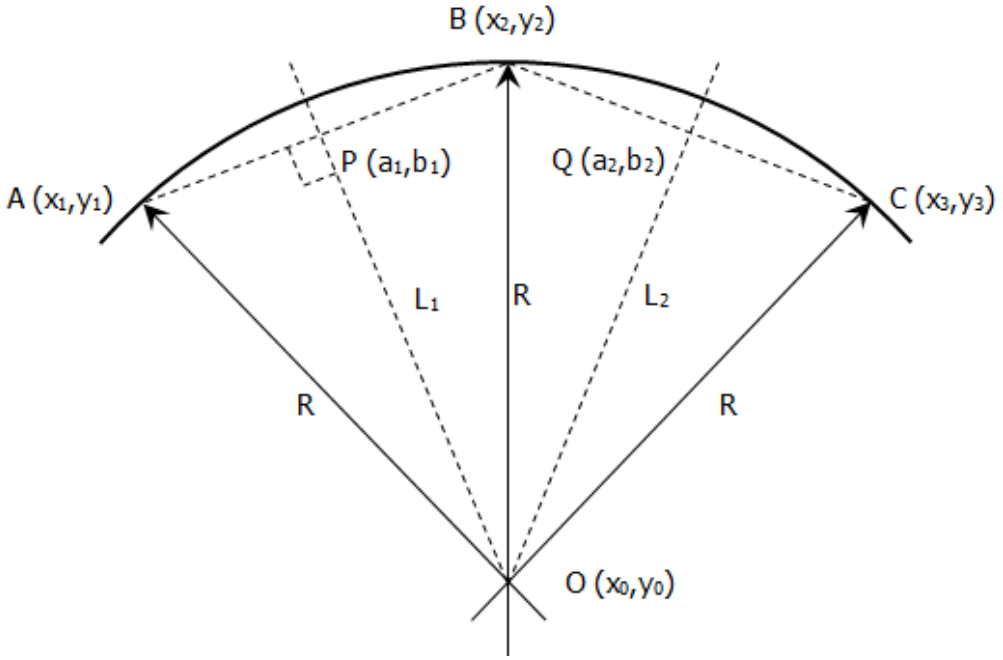

Figure A.1 Curved beam with Three Points

1. Selected any three points on the curved beam. Let Points A, B and C represent three arbitrary points on the finite element model in coordinated system form, A (x_1,y_1) , B (x_2,y_2) and C (x_3,y_3).
2. Calculate Slope and center point of Line AB by following equation;

   Slope of Line AB: $S_{AB} = \frac{y_2 - y_1}{x_2 - x_1}$

   Center point, P: $P(a_1, b_1) = \left(\frac{x_1 + x_2}{2}, \frac{y_1 + y_2}{2}\right)$
3. Calculate slope of L1 which perpendicular to line AB at point P can be expressed as;

   Slope of Line L1: $S_{L1} = -\frac{1}{Slope\ of\ line\ AB} = -\frac{1}{S_{AB}}$
4. Calculate center point of Line BC and slope of L2 by repeat step 2 – 3, but use point B and point C. The equation can be expressed as;

Slope of Line AB: $S_{BC} = \frac{y_3 - y_2}{x_3 - x_2}$

Center point, Q: $Q(a_2, b_2) = \left(\frac{x_2 + x_3}{2}, \frac{y_2 + y_3}{2}\right)$

Slope of Line L2: $S_{L2} = -\frac{1}{Slope\ of\ line\ BC} = -\frac{1}{S_{BC}}$

5. Find the intersection of L1 and L2 which is the center of the curve, point O. The coordinate of point O can be expressed as

$$x_0 = \frac{S_{L1}a_1 - S_{L2}a_2 - b_1 + b_2}{S_{L1} - S_{L2}}$$

$$y_0 = \frac{S_{L1}S_{L2}(a_1 - a_2) - S_{L1}b_1 - S_{L2}b_2}{S_{L1} - S_{L2}}$$

6. Find the distance/radius of the curve ABC, center point to any of the point A, B and C, by the following equation;

$$R = \sqrt{(x_0 - x_1)^2 + (y_0 - y_1)^2} = \sqrt{(x_0 - x_2)^2 + (y_0 - y_2)^2} = \sqrt{(x_0 - x_3)^2 + (y_0 - y_3)^2}$$

APPENDIX B

MATLAB CODE FOR ANALYTICAL SOLUTION

```
%% General Data
la1=[45,-45,0,90,90,0,-45,45];    %Top flange (top layer to bottom)
la2=[45,-45,0,90,90,0,-45,45];    %Bottom flange (top layer to bottom layer)
la3=[45,-45,0,90,90,0,-45,45];    %Web (left layer to right layer)
E1=20.0e6;
E2=1.3e6;
v12=0.23;
G12=1.03e6;
S=[1/E1,-v12/E1,0;-v12/E1,1/E2,0;0,0,1/G12];
Q=inv(S);
%% Applied Load
N_bar_x=0;
M_bar_x=1;
M_bar_z=0;
%% Dimension of Cr0ss-section
bf1=1;   %Width of top flenge (f1)
bf2=1;   %Width of bottom flenge (f2)
hw=1;   %Hight of web (w)
tply=0.005;
%% ABD MATRIX FOR TOP FLANGE
H=fliplr(-numel(la1)*tply/2:tply:numel(la1)*tply/2);
h=transpose(H);
for i=1:numel(la1)
   theta=la1(i);
   m=cosd(theta);
   n=sind(theta);
```

```
    Ts=[m^2,n^2,2*m*n;n^2,m^2,-2*m*n;-m*n,m*n,m^2-n^2];
    Te=[m^2,n^2,m*n;n^2,m^2,-m*n;-2*m*n,2*m*n,m^2-n^2];
    Qbar1(:,:,i)=Ts\Q*Te;
end
A=[0,0,0;0,0,0;0,0,0];
B=[0,0,0;0,0,0;0,0,0];
D=[0,0,0;0,0,0;0,0,0];
for i=1:numel(la1)
    A=A+(Qbar1(:,:,i)*(h(i)-h(i+1)));
    B=B+(Qbar1(:,:,i)*(h(i)^2-h(i+1)^2))/2;
    D=D+(Qbar1(:,:,i)*(h(i)^3-h(i+1)^3))/3;
end
ABD1=[A,B;B,D];
%% ABD MATRIX FOR BOTTOM FLANGE
H=fliplr(-numel(la2)*tply/2:tply:numel(la2)*tply/2);
h=transpose(H);
for i=1:numel(la2)
    theta=la2(i);
    m=cosd(theta);
    n=sind(theta);
    Ts=[m^2,n^2,2*m*n;n^2,m^2,-2*m*n;-m*n,m*n,m^2-n^2];
    Te=[m^2,n^2,m*n;n^2,m^2,-m*n;-2*m*n,2*m*n,m^2-n^2];
    Qbar2(:,:,i)=Ts\Q*Te;
end
A=[0,0,0;0,0,0;0,0,0];
B=[0,0,0;0,0,0;0,0,0];
```

```
D=[0,0,0;0,0,0;0,0,0];
for i=1:numel(la2)
    A=A+(Qbar2(:,:,i)*(h(i)-h(i+1)));
    B=B+(Qbar2(:,:,i)*(h(i)^2-h(i+1)^2))/2;
    D=D+(Qbar2(:,:,i)*(h(i)^3-h(i+1)^3))/3;
end
ABD2=[A,B;B,D];
%% ABD MATRIX FOR WEB
H=fliplr(-numel(la3)*tply/2:tply:numel(la3)*tply/2);
h=transpose(H);
for i=1:numel(la3)
    theta=la3(i);
    m=cosd(theta);
    n=sind(theta);
    Ts=[m^2,n^2,2*m*n;n^2,m^2,-2*m*n;-m*n,m*n,m^2-n^2];
    Te=[m^2,n^2,m*n;n^2,m^2,-m*n;-2*m*n,2*m*n,m^2-n^2];
    Qbar3(:,:,i)=Ts\Q*Te;
end
A=[0,0,0;0,0,0;0,0,0];
B=[0,0,0;0,0,0;0,0,0];
D=[0,0,0;0,0,0;0,0,0];
for i=1:numel(la3)
    A=A+(Qbar3(:,:,i)*(h(i)-h(i+1)));
    B=B+(Qbar3(:,:,i)*(h(i)^2-h(i+1)^2))/2;
    D=D+(Qbar3(:,:,i)*(h(i)^3-h(i+1)^3))/3;
end
```

```
ABD3=[A,B;B,D];
%% Centroid of each sub-laminate
abd1=inv(ABD1);
rho1=-abd1(1,4)/abd1(4,4);
abd2=inv(ABD2);
rho2=-abd2(1,4)/abd2(4,4);
abd3=inv(ABD3);
rho3=-abd3(1,4)/abd3(4,4);
%% Stiffness For Narrow Beam Theory
astar1=abd1(1,1)-abd1(1,6)^2/abd1(6,6);
bstar1=abd1(1,4)-abd1(1,6)*abd1(4,6)/abd1(6,6);
dstar1=abd1(4,4)-abd1(4,6)^2/abd1(6,6);
abdstar1=[astar1,bstar1;bstar1,dstar1];
ABDstar1=inv(abdstar1);

astar2=abd2(1,1)-abd2(1,6)^2/abd2(6,6);
bstar2=abd2(1,4)-abd2(1,6)*abd2(4,6)/abd2(6,6);
dstar2=abd2(4,4)-abd2(4,6)^2/abd2(6,6);
abdstar2=[astar2,bstar2;bstar2,dstar2];
ABDstar2=inv(abdstar2);

astar3=abd3(1,1)-abd3(1,6)^2/abd3(6,6);
bstar3=abd3(1,4)-abd3(1,6)*abd3(4,6)/abd3(6,6);
dstar3=abd3(4,4)-abd3(4,6)^2/abd3(6,6);
abdstar3=[astar3,bstar3;bstar3,dstar3];
ABDstar3=inv(abdstar3);
```

```
%% Geometry of C Beam
tf1=numel(la1)*tply;      %Total thickness of top flange (f1)
tf2=numel(la2)*tply;      %Total thickness of bottom flange (f2)
tw=numel(la3)*tply;       %Total thickness of web (w)
%% Centroid of C cross section in Z-direction
zf1=tf2+hw+tf1/2;         %Distance from most bottom to mid-section of top flange (f1)
zf2=tf2/2;                %Distance from most bottom to mid-section of bottom flange (f2)
zw=tf2+hw/2;              %Distance from most bottom to mid-section of web (w)
zf1c=zf1+rho1;            %Distance from most bottom to centroid of top flange (f1)
zf2c=zf2+rho2;            %Distance from most bottom to centroid of bottom flange (f2)
zwc=zw;                   %Distance from most bottom to centroid of web (w)
%% Centroid of C cross section in Y-direction
yf1=bf1/2;                %Distance from most left to mid-section of top flange (f1)
yf2=bf2/2;                %Distance from most left to mid-section of bottom flange (f2)
yw=tw/2;                  %Distance from most left to mid-section of web (w)
yf1c=yf1;                 %Distance from most left to centroid of top flange (f1) in Y-direction
yf2c=yf2;                 %Distance from most left to centroid of bottom flange (f2) in Y-direction
ywc=yw-rho3;              %Distance from most left to centroid of web (w) in Y-direction
%% Centroid for Isotropic Material in Z and Y direction
Af1=tf1*bf1;
Af2=tf2*bf2;
Aw=tw*hw;
zc=(Af1*zf1+Af2*zf2+Aw*zw)/(Af1+Af2+Aw);
yc=(Af1*yf1+Af2*yf2+Aw*yw)/(Af1+Af2+Aw);
%% Centroid for Composite Material in Z and Y direction
```

```
Zc=(zf1*bf1*ABDstar1(1,1)+zf2*bf2*ABDstar2(1,1)+zw*hw*ABDstar3(1,1))/(bf1*ABDstar1(1,1)+
bf2*ABDstar2(1,1)+hw*ABDstar3(1,1));

Yc=(yf1*bf1*ABDstar1(1,1)+yf2*bf2*ABDstar2(1,1)+yw*hw*ABDstar3(1,1))/(bf1*ABDstar1(1,1)+
bf2*ABDstar2(1,1)+hw*ABDstar3(1,1));
%% Axial Stiffness & Bending Stiffness
% Distance from Centroid/mid-section of each laminate to Centroid of cross-section
% Z-direction
zf1cc=zf1c-Zc;
zf2cc=zf2c-Zc;
zwcc=zwc-Zc;
zf1mc=zf1-Zc;
zf2mc=zf2-Zc;
zwmc=zw-Zc;
% Y-Direction
yf1cc=Yc-yf1c;
yf2cc=Yc-yf2c;
ywcc=Yc-ywc;
yf1mc=Yc-yf1;
yf2mc=Yc-yf2;
ywmc=Yc-yw;

Ax=bf1*ABDstar1(1,1)+bf2*ABDstar2(1,1)+hw*ABDstar3(1,1);

Dx=bf1*(ABDstar1(2,2)+2*zf1cc*ABDstar1(1,2)+zf1cc^2*ABDstar1(1,1))+bf2*(ABDstar2(2,2)+2*
zf2cc*ABDstar2(1,2)+zf2cc^2*ABDstar2(1,1))+(hw^3/12+hw*zwcc^2)*ABDstar3(1,1);
```

```
Dy=(bf1^3/12+bf1*yf1cc^2)*ABDstar1(1,1)+(bf2^3/12+bf2*yf2cc^2)*ABDstar2(1,1)+(hw*(ABDst
ar2(2,2)+2*ywcc*ABDstar3(1,2)+ywcc^2*ABDstar3(1,1)));

Dxy=(ABDstar1(1,1)*zf1cc+ABDstar1(1,2))*bf1*yf1cc+(ABDstar2(1,1)*zf2cc+ABDstar2(1,2))*bf2
*yf2cc+(ABDstar3(1,1)*ywcc+ABDstar3(1,2))*hw*zwcc;

Stiff=[Ax,0,0;0,Dx,Dxy;0,Dxy,Dy];

Csk=inv(Stiff)*[N_bar_x;M_bar_x;M_bar_z];

epXc=Csk(1);
KXc=Csk(2);
KZc=Csk(3);

%% Analysis for Top Laminate
Nxf1=ABDstar1(1,1)*(epXc+zf1mc*KXc+yf1mc*KZc)+ABDstar1(1,2)*KXc;
Mxf1=ABDstar1(1,2)*(epXc+zf1mc*KXc+yf1mc*KZc)+ABDstar1(2,2)*KXc;
Mxyf1=-(abd1(6,1)*Nxf1+abd1(6,4)*Mxf1)/abd1(6,6);

midstrainCarvaturef1=abd1*[Nxf1;0;0;Mxf1;0;Mxyf1];
eKmf1=midstrainCarvaturef1;

e0f1=[eKmf1(1);eKmf1(2);eKmf1(3)];      %Mid-Plane Strains of Top Flange
Kf1=[eKmf1(4);eKmf1(5);eKmf1(6)];       %Mid-Plane Curvatures
```

```
H=fliplr(-numel(la1)*tply/2:tply:numel(la1)*tply/2);
h=transpose(H);
for i=1:numel(la1)
   Stxy1(:,(2*i)-1)=Qbar1(:,:,i)*(e0f1+h(i)*Kf1);
   Stxy1(:,2*i)=Qbar1(:,:,i)*(e0f1+h(i+1)*Kf1);
end
%% Analysis for Bottom Laminate
Nxf2=ABDstar2(1,1)*(epXc+zf2mc*KXc+yf2mc*KZc)+ABDstar2(1,2)*KXc;
Mxf2=ABDstar2(1,2)*(epXc+zf2mc*KXc+yf2mc*KZc)+ABDstar2(2,2)*KXc;
Mxyf2=-(abd2(1,6)*Nxf2+abd2(4,6)*Mxf2)/abd2(6,6);

midstrainCarvaturef2=abd2*[Nxf2;0;0;Mxf2;0;Mxyf2];
eKmf2=midstrainCarvaturef2;

e0f2=[eKmf2(1);eKmf2(2);eKmf2(3)];      %Mid-Plane Strains of Bottom Flange
Kf2=[eKmf2(4);eKmf2(5);eKmf2(6)];       %Mid-Plane Curvatures

H=fliplr(-numel(la2)*tply/2:tply:numel(la2)*tply/2);
h=transpose(H);
for i=1:numel(la2)
   Stxy2(:,(2*i)-1)=Qbar2(:,:,i)*(e0f2+h(i)*Kf2);
   Stxy2(:,2*i)=Qbar2(:,:,i)*(e0f2+h(i+1)*Kf2);
end
%% Analysis for Web Laminate
Nxf3=ABDstar3(1,1)*(epXc+zwmc*KXc+ywmc*KZc)+ABDstar3(1,2)*KZc;
Mxf3=ABDstar3(1,2)*(epXc+zwmc*KXc+ywmc*KZc)+ABDstar3(2,2)*KZc;
```

```
Mxyf3=-(abd3(6,1)*Nxf3+abd1(6,4)*Mxf3)/abd3(6,6);

midstrainCarvaturef3=abd3*[Nxf3;0;0;Mxf3;0;Mxyf3];
eKmf3=midstrainCarvaturef3;

e0f3=[eKmf3(1);eKmf3(2);eKmf3(3)];      %Mid-Plane Strains of Web
Kf3=[eKmf3(4);eKmf3(5);eKmf3(6)];       %Mid-Plane Curvatures

H=fliplr(-numel(la3)*tply/2:tply:numel(la3)*tply/2);
h=transpose(H);
for i=1:numel(la3)
   Stxy3(:,(2*i)-1)=Qbar3(:,:,i)*(e0f3+h(i)*Kf3);
   Stxy3(:,2*i)=Qbar3(:,:,i)*(e0f3+h(i)*Kf3);
end.
```

APPENDIX C

ANSYS 13 BATCH CODES FOR FINITE ELEMENT MODELS

```
/UNITS,BIN
/PREP7
/TRIAD,LBOT
! Define Parameter
L=10
bf1=1
bf2=1
w=1
! Define Key point
K,1,0,0,0
K,2,L,0,0
K,3,L,bf2,0
K,4,0,bf2,0
K,5,0,0,w
K,6,L,0,w
K,7,L,bf1,w
K,8,0,bf1,w
! Dummy point at centroid
K,9,L,0.34,w/2
!Define Area
A,5,6,7,8
A,1,2,3,4
A,1,2,6,5
AGLUE,ALL
/PNUM,AREA,1
! Define New Working plane
```

```
WPROTA,,-90
CSWPLA,11,0
WPROTA,,90
! Define Material Properties
ET,1,SHELL181
KEYOPT,1,3,2
KEYOPT,1,8,2
ET,2,MASS21
R,1
MP,EX,1,20.0e6
MP,EY,1,1.3e6
MP,EZ,1,1.3e6
MP,PRXY,1,0.30
MP,PRYZ,1,0.49
MP,PRXZ,1,0.30
MP,GXY,1,1.03e6
MP,GYZ,1,0.90e6
MP,GXZ,1,1.03e6
MP,CTEX,1,1.0e-6
MP,CTEY,1,30e-6
MP,CTEZ,1,30e-6
! Top flange
SECTYPE,1,SHELL,,TFlange
SECDATA,0.005,1,45,3
SECDATA,0.005,1,-45,3
SECDATA,0.005,1,0,3
```

SECDATA,0.005,1,90,3

SECDATA,0.005,1,90,3

SECDATA,0.005,1,0,3

SECDATA,0.005,1,-45,3

SECDATA,0.005,1,45,3

SECOFFSET,BOTTOM

! Bottom flange

SECTYPE,2,SHELL,,BFlange

SECDATA,0.005,1,45,3

SECDATA,0.005,1,-45,3

SECDATA,0.005,1,0,3

SECDATA,0.005,1,90,3

SECDATA,0.005,1,90,3

SECDATA,0.005,1,0,3

SECDATA,0.005,1,-45,3

SECDATA,0.005,1,45,3

SECOFFSET,TOP

! Web

SECTYPE,3,SHELL,,Web

SECDATA,0.005,1,45,3

SECDATA,0.005,1,-45,3

SECDATA,0.005,1,0,3

SECDATA,0.005,1,90,3

SECDATA,0.005,1,90,3

SECDATA,0.005,1,0,3

SECDATA,0.005,1,-45,3

```
SECDATA,0.005,1,45,3
SECOFFSET,TOP
! Mesh Attribute & SIZE CONTROL & MESH
ASEL,S,AREA,,1
AATT,1,,1,0,1
ASEL,S,AREA,,2
AATT,1,,1,0,2
ASEL,S,AREA,,3
AATT,1,,1,11,3
LSEL,S,LENGTH,,L
LESIZE,ALL,,,L*10,1
LSEL,S,LINE,,2
LSEL,A,LINE,,4
LESIZE,ALL,,,bf1*10,1
LSEL,S,LINE,,6
LSEL,A,LINE,,8
LESIZE,ALL,,,bf2*10,1
LSEL,S,LINE,,9
LSEL,A,LINE,,10
LESIZE,ALL,,,w*10,1
ALLSEL
AMESH,ALL
CSYS,0
KSEL,S,KP,,9
KATT,1,1,2,0
KSEL,S,KP,,9
```

```
KMESH,ALL
NSEL,S,LOC,X,L
CERIG,3132,ALL,ALL,,,,
!Apply Constrain
NSEL,S,LOC,X,0
D,ALL,ALL,0
ALLSEL
!Apply Force
F,3132,FX,1
/SOLU
ANTYPE,STATIC
SOLVE
```

REFERENCES

1. Vasiliev, V.V., 1993, “Mechanics of Composite Structure”, Taylor & Francis, Washington, DC.

2. Barbero, E.J., 1999, “Introduction to Composite Material Design”, Taylor & Francis, Boca Raton, FL.

3. Chan, W.S. and Demirhan, K.C., “A Simple Closed-Fprm Solution of Benging Stiffness for Laminated Composite Tube”, Journal of Reinforced Plastics and Composite,v 19, No. 04, 2000, p 278-291.

4. Su, C.W., “Thermal Stresses of Composite Beams with Rectangular and Tubular Cross-Section” , The University of Texas at Arlington, 2007.

5. Nguyen, T., “Effect of Curvature on The Stresses of A Curved Laminated Beam Subjectd to Bending”, The University of Texas at Arlington, 2010.

6. Syed, K.A. and Chan, W.S., “Analysis of Hat-Sectioned Reinforced Composite Beams”, Proceeding of American Socity for Composite Conference.

7. Jung, S.N., and Lee, J.Y., “Closed-form Analysis of Thin-walled Composite I-beams Considering Non-classical Effects”, Composite Structure Vol.60, 2003, pp. 9-17.

8. Parambil, J.C., “Stress Analysis of Laminated Composite Beam with I-section”, The University of Texas at Arlington, 2010.

9. Rios, G., “A Unified Analysis of Stiffener Reinforced Composite Beams with Arbitrary Cross-section”, The University of Texas at Arlington, 2009.

10. Ugural, A.C. and Fenster, S.K.,2010, Chapter 1 in Advanced Strength and Applied Elasticity, Prenton Hall, New Jersey.

11. Swanson S.R., 1997, “Introduction to Design and Analysis with Advanced Composite Material”, Prentice Hill, Upper Saddle River, New Jersey.

.

BIOGRAPHICAL INFORMATION

Tattchapong Kumton received his B.S.degree in Mechanical Engineering from Royal Thai Air Force Academy, Bangkok, Thailand in 2004. From 2004 to 2010, he was in the Accessory Repair Division, Directorate of Aeronautical Engineering as an air craft's propeller engineer. In 2010, he joined the University of Texas at Arlington in August 2010 for Master's program in Aerospace Engineering and graduated in December 18, 2012.